Table 1 Characteristics of patients with chronic hepatitis C virus (HCV) infection

Subject	Age	Sex	HCV-RNA (KIU)	ALT (U/l)	Treatment duration	SVR
1	43	F	440	17	48 week	SVR
2	56	M	2000	146	48 week	non
3	49	F	1200	31	72 week	SVR
4	49	M	340	106	48 week	SVR
5	65	F	3800	24	72 week	SVR
6	58	M	320	25	48 week	SVR
7	56	M	2551	24	48 week	non
8	55	M	939	43	48 week	SVR
9	46	M	1200	64	48 week	SVR
10	46	M	1059	42	48 week	SVR
11	43	M	407	91	24 week	non
12	63	F	1621	61	48 week	non
13	63	F	1841	63	48 week	non
14	47	M	458	41	48 week	SVR
15	36	M	1024	79	48 week	non
16	61	F	677	148	48 week	non

ALT, alanine aminotransferase; F, female; M, male; non, non-SVR; SVR, sustained virologic response.

by incubation for 2 h with biotinylated mAb anti-human IFN-γ (7-6B-1, Mabtech) at 2 μg/mL. Plates were washed six times and avidin-peroxidase complex (Vectastain Elite Kit, Vector Laboratories, Burlingame, CA) were added for 1 h. Unbound complex was removed by washing and 3-Amino-9-ethylcarbazole substrate (Sigma, St Louis, MO) was added for 5 min. The data are represented as mean IFN-γ spots per 100 000 T cells analyzed.

Statistics

All values were expressed as the mean and standard deviation (SD). The statistical significance of differences between the groups was determined by applying Mann–Whitney *U*-test. We defined statistical significance as $P < 0.05$.

RESULTS

Analysis of HCV derived peptide-specific IFN-γ release of peripheral blood CD8+ T cells in ELISPOT assay

WE ASSESSED PERIPHERAL blood CD8+ T cell responses against HCV derived peptides ($Core_{35-44}$, $Core_{131-140}$, $NS3_{1073-1081}$, $NS3_{1406-1415}$) in 16 HLA-A2+ HCV patients and 6 healthy donors. As shown in Figure 1, the numbers of IFN-γ spots (per 100 000 CD8+ T cells) observed for T cell responses against HCV peptides in pre-IFN patients were as low as those observed in healthy HLA-A2+ donors. In contrast, significant elevations of ELISPOT reactivity to three peptides ($Core_{131-140}$, $NS3_{1073-1081}$, $NS3_{1406-1415}$) were observed in IFN-4week patients compared with healthy donors. The number of IFN-γ spots against $Core_{35-44}$ peptides in IFN-4week patients also tended to be higher than those in healthy donors. In treated HCV patients, the numbers of IFN-γ spots against all four HCV derived peptides in IFN-4week patients were significantly higher than those in pre-IFN patients (Fig. 1). We also examined whether the frequencies of HCV-specific CD8+ T cell responses were associated with sex difference. The frequencies of CTLs against all four peptides were similar between males and females before and 4 weeks after starting treatment (data not shown).

HCV-specific CD8+ T cell responses in pre-IFN patients were not associated with the antiviral activity of the combination therapy of Peg-IFNα-2b plus ribavirin

We examined the association between HCV-specific CD8+ T cell responses in pre-IFN patients and ALT levels or HCV viral load before treatment. No association was observed between the frequencies of HCV-specific CD8+ T cells in pre-IFN patients and ALT levels or HCV viral load of pre-treated patients (Fig. 2).

We next examined whether HCV-specific CD8+ T cell responses in pre-IFN patients were associated with the antiviral activity of this combination therapy. As shown in Figure 3, the frequencies of CD8+ T cell responses against all four HCV proteins-derived peptides in

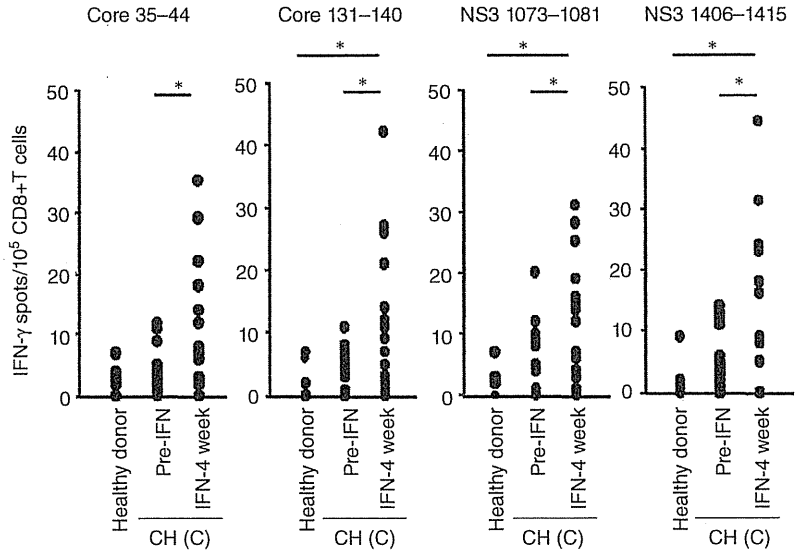

Figure 1 Interferon (IFN)-γ enzyme-linked immunospot (ELISPOT) analysis of hepatitis C virus (HCV)-specific CD8+ T cell responses in HCV patients treated with the combination therapy of peg-IFNα plus ribavirin. Peripheral blood CD8+ T cells were isolated from HLA-A2+ healthy donors and chronic hepatitis C (CH-C) patients. The CH-C patients were treated with the combination therapy of peg-IFNα plus ribavirin and PBMC were isolated from pre-treated patients (Pre-IFN) and treated patients 4 weeks after starting treatment (IFN-4week). HCV-specific CD8+ T cell responses were evaluated by IFN-γ ELISPOT as outlined in "Materials and Methods". Data are reported as IFN-γ spots/ 100 000 CD8+ T cells and represent the mean of triplicate determinations. T cell reactivity against T2.DR4 cells pulsed with HLA-A2-presenting HIV-nef$_{190-196}$ epitope served as the negative control in all cases, and this value was subtracted from all experimental determinations to determine HCV specific spots numbers. Each symbol within a panel represents the response of an individual donor to the indicated HLA-A2-presenting HCV Core- or NS3-peptides. *$P < 0.05$.

pre-IFN patients were not significantly different between SVR, the group of the patients who were observed SVR, and non-SVR, the group of the patients who were not observed SVR. These results suggested that the baseline HCV-specific CD8+ T cell responses in HCV patients were not associated with the antiviral activity of this combination therapy.

Significant early elevation of HCV-specific CD8+ T cell responses were associated with the antiviral activity of the combination therapy of Peg-IFNα plus ribavirin

We examined the association between early elevation of HCV-specific CD8+ T cell responses and the antiviral activity of this combination therapy. We evaluated the frequencies of CD8+ T cell responses against HCV proteins-derived peptides before and 4 weeks after starting treatment. As shown in Figure 4, in SVR patients, the frequencies of CD8+ T cell responses against all four HCV peptides (Core$_{35-44}$, Core$_{131-140}$, NS3$_{1073-1081}$, NS3$_{1406-1415}$) increased significantly 4 weeks after starting treatment. In contrast, the frequencies of CD8+ T cell responses against all four HCV peptides did not increase in non-SVR patients. These results demonstrated that significant early elevation of HCV-specific CD8+ T cell responses were associated with the antiviral activity of this combination therapy.

DISCUSSION

HCV-SPECIFIC CD8+ CTLs have been reported to play a significant role in the elimination of HCV in acute hepatitis of HCV.[4,9] In contrast, in chronic infection of HCV, HCV-specific CD8+ T cell responses were weak and were directed against a limited series of epitopes compared with acute hepatitis.[9] These might cause persistent infection of HCV in the HCV infected host. However, conflicting results have been reported with respect to HCV-specific CD8+ T cell responses on the antiviral activity of IFN therapy. IFNα monotherapy may promote viral clearance by enhancing the host CTL responses.[14,15] But Rehermann et al. reported that CTL

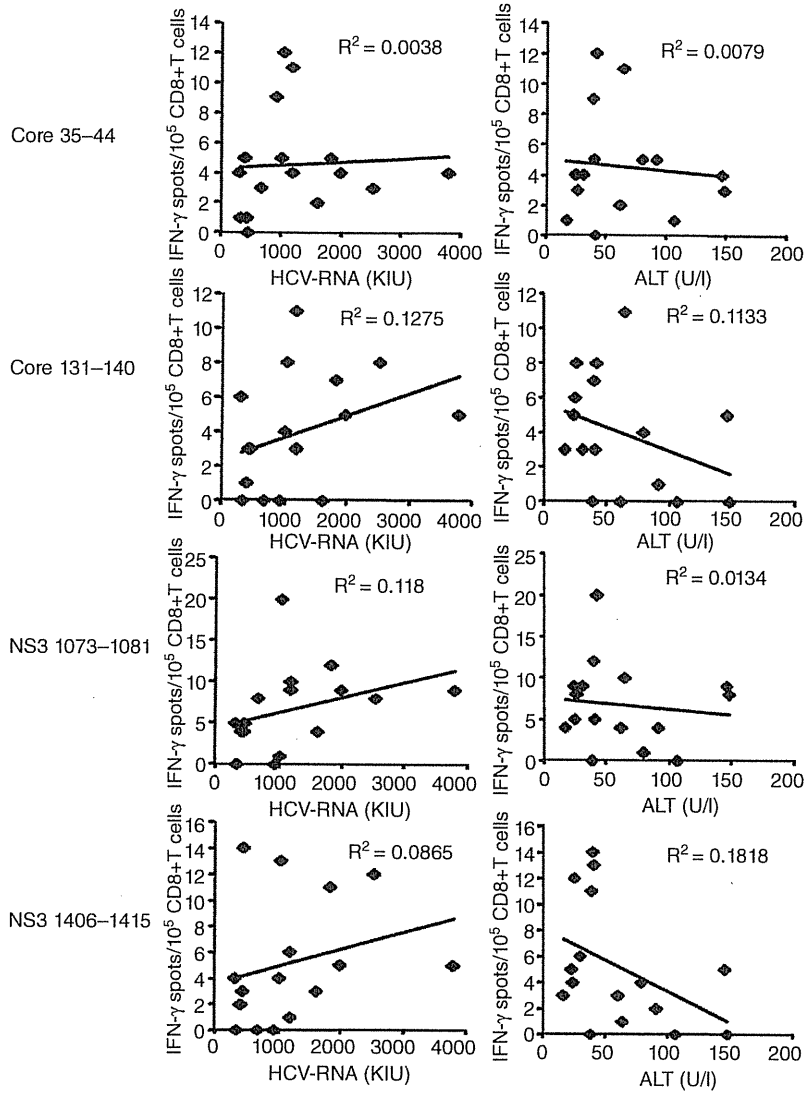

Figure 2 The association between the hepatitis C virus (HCV)-specific CD8+ T cell responses of pre-IFN patients and the serum alanine aminotransferase (ALT) levels or the HCV viral load of patients before treatment. The frequencies of HCV Core and NS3 proteins-derived peptides specific CD8+ T cell responses in pre-IFN HCV patients were evaluated by interferon (IFN)-γ enzyme-linked immunospot (ELISPOT). We examined the association between the frequencies of HCV Core and NS3 proteins-derived peptides specific CD8+ T cell responses in pre-IFN HCV patient and the serum ALT levels or HCV viral loads of patients before treatment.

precursor frequencies against a range of HCV epitopes did not change during or after the course of IFNα monotherapy.[13] Recently, the combination therapy of PegIFNα plus ribavirin is standard treatment in the treatment of HCV infected patients with the better results of viral clearance compared with IFNα monotherapy. This suggested that this combination therapy might modify the HCV specific CD8+ T cell responses. We evaluated HCV-specific CD8+ T cell responses by IFN-γ ELISPOT assay, a functional assay of T cells. Significant increase of the frequencies of HCV-specific CD8+ T cells between pre-IFN and IFN-4week could be observed in SVR patients, but not in non SVR patients. This is consistent with the previous report of evaluating the frequencies of HCV-specific CTLs by direct ex vivo staining with HCV-specific pentamers.[16] Thus the evaluation of reactivity against HCV Core and NS3 proteins-derived peptides might be useful in predicting the clinical outcome of this combination therapy.

It has been reported that complete early virologic response (cEVR), which means HCV RNA negativity at week 12, is strongly related to SVR in the combination therapy of Peg-IFNα plus ribavirin.[12,17] cEVR itself has been reported to be an independent predictive factor of

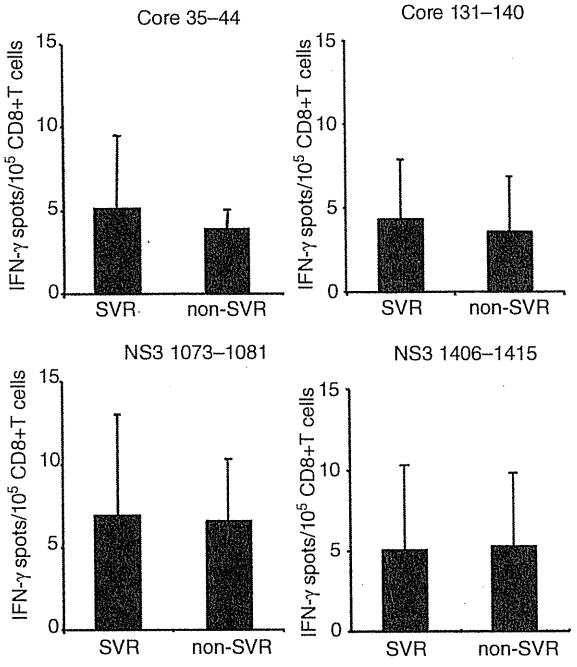

Figure 3 Comparison of the frequencies of hepatitis C virus (HCV)-specific CD8+ T cells in pre-treated HCV patients between sustained virologic response (SVR) and non-SVR. HCV Core and NS3 proteins-derived peptides specific CD8+ T cell responses in pre-treated HCV patients were evaluated by interferon (IFN)-γ enzyme-linked immunospot (ELISPOT). We analyzed the association between the HCV-specific CD8+ T cell responses and the achieving of SVR. SVR: patients who were observed SVR, non-SVR: patients who were not observed SVR.

SVR.[1,12] We also examined the association between cEVR and early elevation of HCV-specific CD8+ T cell responses. The frequencies of CD8+ T cell responses against all four HCV derived peptides in pre-IFN patients were not significantly different between cEVR and non-cEVR (Tatsumi T, unpublished data). In cEVR patients, the frequencies of CD8+ T cell responses against three HCV peptides $Core_{35-44}$, $Core_{131-140}$, $NS3_{1406-1415}$) increased significantly 4 weeks after the starting treatment and those against $NS3_{1073-1081}$ peptide tended to increase although these were not significant. In contrast, the frequencies of CD8+ T cell responses against all four HCV peptides did not increase in non-cEVR patients (Tatsumi T, unpublished data). The cEVR results were almost similar to those of the SVR results. Although we could not evaluate the HCV RNA levels at 4 week after starting treatment, the cEVR results suggested that early elevation of the frequencies of HCV-specific CD8+ T cell responses might reflect the decrease of viral load of HCV.

CD8+ CTL activities in pre-treated HCV patients have been reported to be very low.[7,18,19] Consistent with the previous observations, the frequencies of HCV specific CD8+ T cell in pre-treated patients were also low in our study. The frequencies of HCV-specific CD8+ T cells in pre-treated patients were not associated with the HCV viral load and the serum ALT levels of patients before treatment. Several reports demonstrated that the baseline presence of HCV-specific CTLs prior to treatment was associated with viral clearance.[7,18] However, the frequencies of HCV-specific CD8+ T cells in pre-treated patients were not associated with the achievement of SVR in our study. In previous other reports, whole PBMC isolated from treated patients were used to evaluate the antiviral activity of HCV-specific CD8+ T cells. In our study, enriched CD8+ T cells obtained by magnetic sorting methods were used to enhance the sensitivity for the detection of HCV-specific CD8+ T cells. Both ELISPOT and staining with tetramers/pentamers could be applied for immunological monitoring for peptide-specific CTLs.[20] ELISPOT can detect activated functional CTLs, and tetramers/pentamers staining can detect peptide-specific CTLs.[20] In our study, we assessed the HCV-specific CD8+ T cell responses by IFN-γ ELISPOT, which is the most well-established methods and has already applied for immunological monitoring in cancer patients.[11] Recently perforin- or granzyme B-ELISPOT assays have also been reported. However, due to limitations in cell numbers of PBMC isolated from HCV patients, we were unable to apply another system of immunological monitoring and test other functional molecules. If we can apply these ELISPOT assays, we could directly evaluate the cytotoxic activity of HCV-specific CTLs.

In our study, the frequencies of HCV-specific CD8+ T cells in pre-treated patients were similar between SVR and non-SVR patients. In contrast, significant increase of the frequencies of HCV-specific CD8+ T cells between pre-IFN and IFN-4week could be observed in SVR patients, but not in non SVR patients. Caetano et al. evaluated the HCV-specific CD8+ T cells by HLA class I pentamers specific for the one HCV-Core epitope and one NS3 epitope which were same as we used.[16] They demonstrated that the increase of the frequencies of HCV-specific CTLs at 1 month after starting treatment was mainly due to terminally differentiated cells as well as, to a lesser extent, central memory cells in SVR patients and, in contrast, the increase of HCV-specific

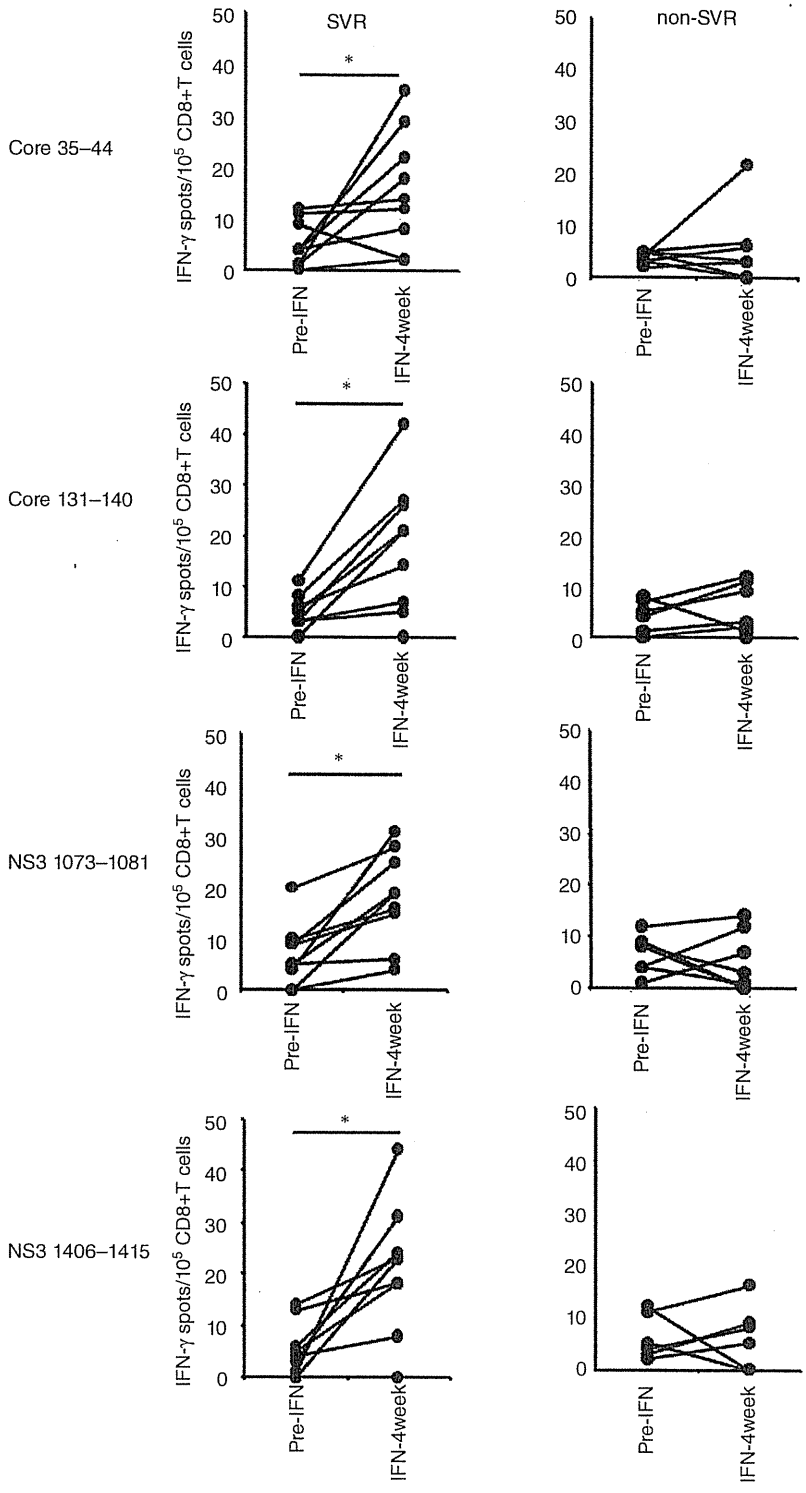

Figure 4 Analysis of the association of the change of hepatitis C virus (HCV)-specific CD8+ T cell responses between pre-IFN and IFN-4week chronic hepatitis C (CH-C) patients with the achieving sustained virologic response (SVR). Peripheral blood CD8+ T cells were isolated from pre-IFN and IFN-4week patients. HCV-specific CD8+ T cell responses were evaluated by interferon (IFN)-γ enzyme-linked immunospot (ELISPOT) assay. We analyzed the association of HCV-specific CD8+ T cell responses in treated CH-C patients with the achieving SVR. Each symbol within a panel represents the response of an individual donor to the indicated HLA-A2-presenting HCV Core or NS3 protein-derived peptides. The treated patients were divided into two groups; SVR group and non-SVR group. $^*P < 0.05$.

pre-terminally differentiated CD8+ T cells was also observed in non-SVR patients.[16] These results suggested that CTLs maturation efficiently occurred in SVR patients. HCV or HCV-gene products have been reported to inhibit the maturation pathway of CTLs.[5,21] Thus the decrease of viral load during this combination therapy may induce CTL maturation.

We demonstrated that the achievement of SVR in this combination therapy was associated with the early elevation of HCV-specific CD8+ T cell responses, but not with the pre-treated levels of HCV-specific CD8+ T cell responses. These results suggested, at least, that the enhancement of HCV-specific CD8+ T cell responses might play critical roles in the second slope of viral clearance by this combination therapy. The increasing frequencies of HCV-specific CD8+ T cells have also been reported to be associated with SVR during the combination therapy by evaluating with pentamers of HCV-specific peptides.[16] Ribavirin has immunomodulatory effect with a switch from Th2 to Th1 cytokine profile.[22] The combined use of pegIFNα and ribavirin might have more immunomodulatory effect to generate HCV specific CTLs. However, even now, this should be elucidated to develop better treatment of chronic hepatitis C.

Although CTL responses to HCV are multi-specific,[13,23] we and others tested only small part of the known CTL epitopes of HCV, which do not comprise all potential HLA A2-restricted CTL epitopes of HCV. HCV may have mutated and escaped from the CTL responses to the corresponding epitopes in the chronically infected patients. The epitopes used in our study have been applied to the detection of HCV-specific CTLs in several other previous studies,[5,15,16] which support the usefulness of the selected epitopes. Our results demonstrated that the increases of the frequencies of CD8+ T cells against four synthesized peptides were associated with the antiviral activity of this combination therapy. Thus the selected epitopes used in our experiments were probably stable, at least, during the 4 weeks after starting treatment.

In spite of recent progress for HCV treatment, there remains significant room for improvement. To date, a variety of viral factors and host factors that correlate with SVR in the combination therapy have been noted. Recently, in addition to viral factors and host factors, response and adherence to treatment have been noted.[2] To establish the better treatment, the detail mechanism of HCV elimination should be elucidated. In the present study, we demonstrated that early enhancement of HCV-specific CD8+ T cell responses was associated with the achieving SVR in this combination therapy. These suggest that activation of antiviral CTLs might be involved in the elimination of HCV. The early elevation of HCV-specific CTL responses in treated HCV patients may be a candidate for predicting SVR in this combination therapy.

ACKNOWLEDGEMENTS

THE FORMER INSTITUTION of Nakazuru S and Mita E was Saiseikai-Senri Hospital (Suita, Japan). This work was supported by a Grant-in-Aid from the Ministry of Education, Culture, Sports, Science and Technology of Japan (Hiramatsu N) and a Grant-in-Aid from Viral Hepatitis Research Foundation of Japan (Tatsumi T).

REFERENCES

1 Kumada H, Okanoue T, Onji M *et al.* Guidelines for the treatment of chronic hepatitis and cirrhosis due to hepatitis C virus infection for the fiscal year 2008 in Japan. *Hepatol Res* 2010; **40**: 8–13.
2 Hayashi N, Takehara T. Antiviral therapy for chronic hepatitis C: past, present, and future. *J Gastroenterol* 2006; **41**: 17–27.
3 Price DA, Klenerman P, Booth BL, Phillip RE, Sewell AL. Cytotoxic T lymphocytes, chemokines and antiviral immunity. *Annu Rev Immunol* 1999; **14**: 207–32.
4 Gruener NH, Lechner F, Jung MC *et al.* Sustained dysfunction of antiviral CD8+ T lymphocytes after infection with hepatitis C virus. *J Virol* 2001; **75**: 5550–8.
5 Wedemeyer H, He XS, Nascimbeni M *et al.* Impaired effector function hepatitis C virus-specific CD8+ T cells in chronic hepatitis C virus infection. *J Immunol* 2002; **169**: 3447–58.
6 Takaki A, Wiese M, Maertens G *et al.* Cellular immune responses persist, humoral responses decrease two decade after recovery from a single source outbreak of hepatitis C. *Nat Med* 2000; **6**: 578–82.
7 Pilli M, Zerbini A, Penna A *et al.* HCV-specific T-cell response in relation to viral kinetics and treatment outcome (DITTO-HCV project). *Gastroenterology* 2007; **133**: 1132–43.
8 Ishii S, Koziel MJ. Immune responses during acute and chronic infection with hepatitis C virus. *Clin Immunol* 2008; **128**: 133–47.
9 Altman JD, Moss PAH, Goulder PJR *et al.* Phenotypic analysis of antigen-specific T lymphocytes. *Science* 1996; **274**: 94–6.
10 Lalvani A, Brookes R, Hambleton S, Britton WJ, Hill AV, McMicheal AJ. Rapid effector function in CD8+ memory T cells. *J Exp Med* 1997; **186**: 859–65.
11 Tatsumi T, Herrem CJ, Olson WC *et al.* Disease stage variation in CD4+ and CD8+ T-cell reactivity to the receptor

tyrosine kinase EphA2 in patients with renal cell carcinoma. *Cancer Res* 2003; **63**: 4481–9.
12 Oze T, Hiramatsu N, Yakushijin T *et al.* Pegylated interferon alpha-2b (Peg-IFN α-2b) affects early virologic response dose-dependently in patients with chronic hepatitis C genotype 1 during treatment with Peg-IFN α-2b plus ribavirin. *J Viral Hepat* 2009; **16**: 578–85.
13 Rehermann B, Chang KM, McHutchinson JG, Kokka R, Houghton M, Chisari FV. Quantitative analysis of the peripheral blood cytotoxic T lymphocytes response in patients with chronic hepatitis C virus infection. *J Clin Invest* 1996; **98**: 1432–40.
14 Nelson DR, Marousis CG, Ohno T, Davis GL, Lau JY. Intrahepatic hepatitis C virus-specific cytotoxic T lymphocytes activity and response to interferon alfa therapy in chronic hepatitis C. *Hepatology* 1998; **28**: 225–30.
15 Lohr HF, Schmitz D, Arenz M, Weyer S, Gerken G, Meyer zum Buschenfelde KH. The viral clearance in interferon-treated chronic hepatitis C is associated with increased cytotoxic T cell frequencies. *J Hepatol* 1999; **31**: 407–15.
16 Caetano J, Martinho A, Paiva A, Pais B, Valente C, Luxo C. Differences in hepatitis C virus (HCV)-specific CD8 T-cell phenotype during pegylated alpha interferon and ribavirin treatment are related to response to antiviral therapy in patients chronically infected with HCV. *J Virol* 2008; **82**: 7567–77.
17 Fried MW, Schifman ML, Reddy KR *et al.* Peginterferon alpha-2a plus ribavirin for chronic hepatitis C virus infection. *N Eng J Med* 2002; **347**: 975–82.
18 Freeman AJ, Marinos G, Ffrench RA, Lloyd AR. Intrahepatic and peripheral blood virus-specific cytotoxic T lymphocyte activity is associated with a response to combination IFN-α and ribavirin treatment among patients with chronic hepatitis C virus infection. *J Viral Hepat* 2005; **12**: 125–9.
19 Barnes E, Harcourt G, Brown D *et al.* The dynamics of T-lymhocyte responses during combination therapy for chronic hepatitis C virus infection. *Hepatology* 2002; **36**: 743–54.
20 Sato N, Hirohashi Y, Tsukahara T *et al.* Molecular pathological approaches to human tumor immunology. *Pathol Int* 2009; **59**: 205–17.
21 Lechner W, Wong DK, Dubar PR *et al.* Analysis of successful immune responses in persons infected with hepatitis C virus. *J Exp Med* 2000; **191**: 1499–512.
22 Tam RC, Pai B, Bard J *et al.* Ribavirin polarizes human T cell responses toward a type 1 cytokine profile. *J Hepatol* 1999; **30**: 376–82.
23 He XS, Rehermann B, Lopez-Labradoe XL *et al.* Quantitative analysis of chronic hepatitis C virus-specific CD8+ T cells in peripheral blood and liver using peptide-MHC tetramers. *Proc Natl Acad Sci USA* 1999; **96**: 5692–7.

Biochemical and Biophysical Research Communications xxx (2011) xxx–xxx

Contents lists available at SciVerse ScienceDirect

Biochemical and Biophysical Research Communications

journal homepage: www.elsevier.com/locate/ybbrc

55 Amino acid linker between helicase and carboxyl terminal domains of RIG-I functions as a critical repression domain and determines inter-domain conformation

Maiko Kageyama [a,b], Kiyohiro Takahasi [a,c], Ryo Narita [a], Reiko Hirai [a,d], Mitsutoshi Yoneyama [a,b,d,e], Hiroki Kato [a,b], Takashi Fujita [a,b,*]

[a] Laboratory of Molecular Genetics, Institute for Virus Research, Kyoto University, Kyoto, Japan
[b] Laboratory of Molecular Cell Biology, Graduate School of Biostudies, Kyoto University, Kyoto, Japan
[c] Institute for Innovative NanoBio Drug Discovery and Development, Graduate School of Pharmaceutical Science, Kyoto University, Kyoto, Japan
[d] Medical Mycology Research Center, Chiba University, Chiba, Japan
[e] PRESTO, Japan Science and Technology Agency, Saitama, Japan

ARTICLE INFO

Article history:
Received 21 September 2011
Available online xxxx

Keywords:
RIG-I
Virus
Interferon

ABSTRACT

In virus-infected cells, viral RNA with non-self structural pattern is recognized by DExD/Hbox RNA helicase, RIG-I. Once RIG-I senses viral RNA, it triggers a signaling cascade, resulting in the activation of genes including type I interferon, which activates antiviral responses. Overexpression of N-terminal caspase activation and recruitment domain (CARD) is sufficient to activate signaling; however basal activity of full-length RIG-I is undetectable. The repressor domain (RD), initially identified as a.a. 735–925, is responsible for diminished basal activity; therefore, it is suggested that RIG-I is under auto-repression in uninfected cells and the repression is reversed upon its encounter with viral RNA. In this report, we further delimited RD to a.a. 747–801, which corresponds to a linker connecting the helicase and the C-terminal domain (CTD). Alanine substitutions of the conserved residues in the linker conferred constitutive activity to full-length RIG-I. We found that the constitutive active mutants do not exhibit ATPase activity, suggesting that ATPase is required for de-repression but not signaling itself. Furthermore, trypsin digestion of recombinant RIG-I revealed that the wild-type, but not linker mutant conforms to the trypsin-resistant structure, containing CARD and helicase domain. The result strongly suggests that the linker is responsible for maintaining RIG-I in a "closed" structure to minimize unwanted production of interferon in uninfected cells. These findings shed light on the structural regulation of RIG-I function.

1. Introduction

Innate immune responses are initiated upon detection of microorganisms such as viruses and bacteria. With no exception, viruses replicate inside the host cells; therefore, detection of viral components within infected cells is the critical step for triggering primary immune responses [1–4]. Viral RNA with a non-self structural signature is sensed by RIG-I-Like Receptor (RLR), which includes RIG-I, MDA5 and LGP2 [5,6]. Sensing viral RNA triggers a cascade of signaling events, leading to the activation of genes, including those encoding type-I interferon (IFN) and proinflammatory cytokines, which in turn participate in the antiviral response.

RIG-I is activated by double-stranded (ds)RNA and its detection is markedly enhanced if tri-phosphate moiety is present at the 5′ end of the RNA [7,8]; therefore, RIG-I acts as a specific sensor of viral dsRNA with 5′-ppp. RIG-I is composed of three functional domains: N-terminal caspase activation and recruitment domain (CARD, a.a. 1–190), RNA helicase domain (a.a. 218–746) and C-terminal domain (CTD, a.a. 802–925). Initial analyses revealed that CARD is essential and sufficient for signaling: over-expression of CARD alone is sufficient for signaling and RIG-I devoid of CARD acts as a dominant inhibitor of signaling. The observation that full-length RIG-I exhibits significantly low basal signaling activity compared to CARD alone led to the hypothesis of auto-repression, in which repressor domain (RD) masks CARD. Deletion mapping revealed that a.a. 735–925 acts as RD [9]. A similar region of LGP2 (a.a. 489–543) but not that of MDA5 exhibits repression function [9].

Abbreviations: RLR, RIG-I-like receptor; RIG-I, retinoic acid-inducible gene I; MDA5, melanoma differentiation-associated gene 5; LGP2, laboratory of genetics and physiology 2; IFN, interferon; dsRNA, double-stranded RNA; CARD, caspase activation and recruitment domain; CTD, C-terminal domain; IPS-1, IFN-β promoter stimulator 1; IRF-3, interferon regulatory factor-3; NF-κB, nuclear factor-κB; SeV, sendai virus; poly (I:C), polyinosinic:polycytidylic acid.

* Corresponding author at: Laboratory of Molecular Genetics, Institute for Virus Research, Kyoto University, Kyoto 606-8507, Japan. Fax: +81 75 751 4031.
E-mail address: tfujita@virus.kyoto-u.ac.jp (T. Fujita).

0006-291X/$ - see front matter © 2011 Elsevier Inc. All rights reserved.
doi:10.1016/j.bbrc.2011.10.015

Please cite this article in press as: M. Kageyama et al., 55 Amino acid linker between helicase and carboxyl terminal domains of RIG-I functions as a critical repression domain and determines inter-domain conformation, Biochem. Biophys. Res. Commun. (2011), doi:10.1016/j.bbrc.2011.10.015

The repression of full-length RIG-I can be liberated upon its encounter with viral RNA. Thus, the de-repression mechanism is critical for the function of RIG-I for acting as a sensor and a switch for signaling. CTD binds to dsRNA with its basic cleft [10]; thus, its involvement in RNA recognition is suggested. It is presumed that the helicase domain also participates in viral RNA recognition, since full-length RIG-I exhibits higher RNA binding affinity [10,11]. Binding of dsRNA induces ATPase activity of RIG-I in vitro. ATPase-deficient RIG-I acts as a dominant inhibitor [5], suggesting that ATP binding and/or its hydrolysis is a critical step in de-repression. RIG-I is a functional RNA helicase, which consumes ATP for dsRNA unwinding [10]; however, dsRNA substrates resistant to RIG-I helicase activity, but not those susceptible, induce IFN production, suggesting that dsRNA unwinding is not critical for signaling. Therefore it is hypothesized that ATPase activity of RIG-I induces a conformational change, resulting in unmasking CARD. Once CARD is liberated, RIG-I may undergo oligomeric complex formation [9]. The oligomer also recruits another CARD-containing adaptor, IPS-1 (IFN-β promoter stimulator 1) (also known as MAVS, VISA and Cardif, [12–15]). IPS-1 is a unique signaling adaptor, expressed on the outer membrane of mitochondria, and its specific localization is critical for its function [13]. IPS-1 transmits a signal through TRAF proteins, resulting in transcription factors IRF-3, IRF-7 and NF-κB, which are responsible for the activation of IFN and cytokine genes [16].

Repression of RIG-I in uninfected cells is crucial for tight regulation of the host immune system and prevents unwanted production of IFN under ordinary conditions; however, the precise mechanism of auto-repression is not known and there is no evidence for the existence of "active" and "inactive" conformations. In the current study, we further delimited RD to the 55 amino acid linker between the helicase domain and CTD. Mutant RIG-I containing amino acid substitutions within the linker conferred constitutive activity. Furthermore, trypsin digestion of wild-type and mutant RIG-I revealed a distinct conformation, suggesting that the mutation inactivated RD and induced an "open" conformation. These findings shed light on the role of RD in RIG-I regulation.

2. Materials and methods

2.1. Cell culture

HEK293T, Huh7.5 and Huh7 cells were maintained in Dulbecco's modified Eagle's medium (DMEM) supplemented with 10% fetal bovine serum (FBS) and 1% penicillin–streptomycin.

2.2. Plasmid construction

All RIG-I full-length mutant constructs used in this study were generated with Prime Star (R) HS DNA Polymerase (TAKARA, Shiga, Japan) or the KOD-Plus Mutagenesis Kit (TOYOBO LIFE SCIENCE, Osaka, Japan), using primers containing the desired mutation, and were sequenced using an ABI 3130xl automatic DNA sequencer to verify the presence of the mutation.

2.3. Protein sequence alignment

Multiple protein sequence alignment was performed using the ClustalX program [17]. DSC, MLRC, and PHD methods were used to predict the protein secondary structure of the linker sequences on the NPS@ (Network Protein Sequence Analysis) server [18].

2.4. Protein purification

The cDNA encoding fusion protein, consisting of Flag-tag and human RIG-I or mutants, was inserted into pAcGHLT-B vector (BD Biosciences, CA, USA), which has GST and His-tag, between NcoI and SmaI sites. To obtain recombinant baculoviruses, SF9 insect cells were co-transfected with the expression plasmid and BD Baculo Gold Linearized Baculovirus DNA (BD Biosciences) according to the manufacturer's protocol. Recombinant virus was recovered from the culture supernatant. The recombinant RIG-I proteins were expressed in Sf9 or High five insect cells (2×10^7 cells/150 mm dish) by infection with recombinant baculovirus (moi 10) for 4 days. The cells were lysed in lysis buffer (50 mM Tris–HCl pH 8.0, 150 mM NaCl, 1.5 mM DTT, 1% Triton X-100) with protease inhibitor cocktail (Nacalai Tesque, Kyoto, Japan). The lysates were centrifuged at 15,000 rpm for 20 min. The supernatants were mixed with Ni-NTA super-flow (QIAGEN, Hilden, Germany) and the beads were washed with binding buffer (20 mM imidazole, 50 mM Tris–HCl pH 8.0, 150 mM NaCl, 1.5 mM DTT). Proteins were eluted with elution buffer 1 (500 mM imidazole, 50 mM Tris–HCl pH 8.0, 150 mM NaCl, 1.5 mM DTT). The eluted protein was further purified with glutathione Sepharose 4B (GE Healthcare, Little Chalfont, Buckinghamshire, UK). Bound proteins were washed with wash buffer (50 mM Tris–HCl pH 8.0, 150 mM NaCl, 1.5 mM DTT) and eluted with elution buffer 2 (50 mM Tris–HCl pH 8.0, 150 mM NaCl, 20 mM glutathione).

2.5. Immunoblot analysis

Huh7.5 cells were seeded in a 6 cm dish (5×10^5 cells/dish/2 ml medium). Before transfection, culture medium was replaced with serum-free DMEM. Expression plasmid for RIG-I wt or mutants (2 μg) was mixed with 1 ml DMEM and 5 μl polyethylenimine Max (Polysciences, Warrington, PA, USA), and then incubated for 15 min. The mixture was added to the culture. After incubation for 1 h, FBS was added to a final concentration 10%. After harvest, whole cell lysate was prepared with NP40 lysis buffer and subjected to Native PAGE or SDS PAGE as described previously [6,19].

2.6. ATPase assay

Reaction mixture (25 μl: 1 μg purified recombinant RIG-I protein, 100 ng RNA, 20 mM Tris–HCl pH 8.0, 1.5 mM $MgCl_2$, 1.5 mM DTT, 20 units Protector RNase Inhibitor, 1 mM ATP) was incubated at 37 °C for 30 min. The product, inorganic phosphate, was quantified using BioMol Green (Enzo, Farmingdale, NY, USA).

2.7. RNA

25 bp dsRNA was prepared by annealing chemically synthesized complementary RNA (p25/25) as described previously [10]. Then, 5′-triphosphate-containing RNA was synthesized using a DNA template and T7 RNA polymerase as described previously [10] as 5′pppGG25, presumably containing copy-back 3′end. Poly (I:C) pull down assay was performed as described previously [5].

2.8. RNA binding assay

Purified GST-fused RIG-I proteins (5 μg) were mixed with the indicated RNAs (0.1 μg) in a 20 μl reaction mixture (20 mM Tris–HCl pH 8.0, 1.5 mM $MgCl_2$, 1.5 mM DTT) and incubated at 37 °C for 15 min. The mixture was resolved by 15% native PAGE. The gel was stained with EtBr to visualize free RNA and protein/RNA complex.

Please cite this article in press as: M. Kageyama et al., 55 Amino acid linker between helicase and carboxyl terminal domains of RIG-I functions as a critical repression domain and determines inter-domain conformation, Biochem. Biophys. Res. Commun. (2011), doi:10.1016/j.bbrc.2011.10.015

2.9. Luciferase reporter assay

Huh7.5 or Huh7 cells were seeded in a 12-well plate (5×10^4 cells/well/0.5 ml medium). Then, 2 μg p-125 Luc IFN-β luciferase reporter plasmid, 20 ng pRL-tk, and 4 μg expression plasmid for RIG-I wt or mutants were mixed with 150 μl Opti-MEM and 9 μl Fugene 6 (Roche), and incubated for 15 min. The mixture was dispensed into 3 wells (50 μl/well). After 20 h of incubation, cells in each well were split into two wells for virus infection. After cells had attached to the dish, one well was mock treated and the other well was infected with SeV (moi 1) for 20 h. Cells were subjected to a Dual-Luciferase (R) Reporter Assay System (Promega, Madison, WI, USA). Luciferase activity was normalized using Renilla luciferase activity (pRL-tk) as a reference. The values show relative

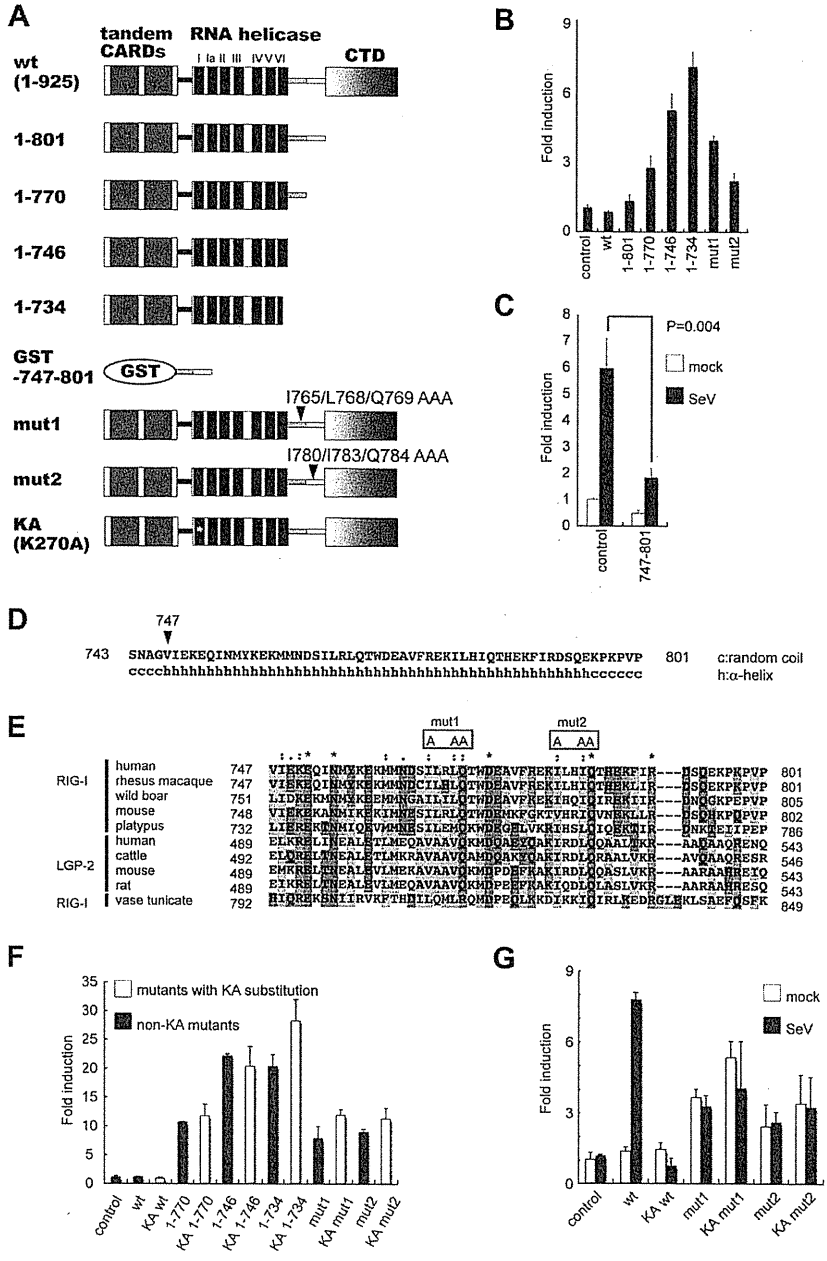

Fig. 1. RIG-I 747-801 is the minimal repression domain. (A) Domain structure of the RIG-I constructs used in this study. The amino acid region encoded by each construct is shown on the left. Mutations are indicated by arrows. (B and C) Activation of IFN-β promoter by RIG-I wt and mutants. Huh7.5 (B) or Huh7 cells (C) were transfected with indicated expression vectors, IFN-β luciferase reporter and pRL-tk as the internal control. In C, 52 h after transfection, cells were infected with Sendai virus (SeV) for 20 h. 24 h (B) or 72 h (C) after transfection, the cells were harvested, and cell lysates were subjected to dual luciferase assay. The values (*Y* axis) show relative luciferase activity as fold induction normalized by the value of unstimulated cells transfected with empty vector (control) for each experiment. Data represent the mean ± standard deviations (SD) ($n = 3$). (D) Predicted secondary structure of the linker of RIG-I. (E) Multiple sequence alignment of the linker of RIG-I and LGP2 from different species. The sequences were aligned using the ClustalX program. Invariant residues are marked with an asterisk. Highly conserved residues are marked with a colon. Similar residues are marked with a dot. Residues targeted for mutation are indicated at the top and were substituted with alanine, indicated as A. (F and G) The effect of ATP binding site mutation on the activity of RIG-I and mutants. Huh7.5 cells were transfected with the indicated expression vectors in the presence of the luciferase reporter and pRL-tk, as in (B). KA: K270A mutation, which disrupts ATP binding motif. 24 h (F) or 72 h (G) after transfection, the cells were harvested. Constitutive activity (F) or SeV induced activity (G) was determined.

Please cite this article in press as: M. Kageyama et al., 55 Amino acid linker between helicase and carboxyl terminal domains of RIG-I functions as a critical repression domain and determines inter-domain conformation, Biochem. Biophys. Res. Commun. (2011), doi:10.1016/j.bbrc.2011.10.015

luciferase activity as fold induction normalized by the value of unstimulated cells transfected with empty vector (control) for each experiment.

2.10. Trypsin digestion

The reaction mixture (10 μl) contained 0.5 picomoles of GST-RIG-I or GST-RIG-I mutants in elution buffer 2. Five nanograms of trypsin (TPCK-treated) was added to the mixture and incubated at 37 °C for 20 min. The reaction was terminated by adding SDS loading buffer (Nacalai Tesque, Kyoto, Japan) (10 μl) and boiling for 1 min. The digestion products were analyzed by SDS–PAGE (5–20% acrylamide gradient) followed by silver staining or Western blotting using monoclonal ANTI-FLAG M2 antibody.

3. Results

3.1. Delimitation of RIG-I repressor domain

Previously, the region of RIG-I encompassing a.a. 735–925 was mapped as RD [9]. Deletion of a.a. 735–925 results in constitutive active RIG-I. Moreover, RD is sufficient to repress virus-induced activation of endogenous RIG-I when a.a. 735–925 alone is over expressed. a.a. 735–925 encompasses the entire CTD (a.a. 802–925), which was defined as a structural domain by a protease digestion experiment and contains the RNA-binding basic cleft [10], and a linker (a.a. 747–801) connecting the helicase domain and the CTD (Fig. 1A). To delimit the functional RD further, we prepared detailed deletion mutants of RIG-I and examined their stimulatory activity on IFN-β luciferase reporter (Fig. 1A and B). Without viral stimulus, wt RIG-I exhibited no stimulatory activity. Consistent with the previous report [9], RIG-I1-734 exhibited marked activation of the reporter. Interestingly, RIG-I1-801, which lacks the entire CTD, exhibited little activity; however, partial and complete deletion of the linker (1–770 and 1–746, respectively) exhibited enhanced reporter activity (Fig. 1B), suggesting that the linker is the minimal repression domain. We genarated a GST fusion construct, GST-RIG-I 747-801, in which the linker was connected with GST. Cells expressing GST as a control showed elevated IFN-β promoter activity upon SeV infection which selectively activates RIG-I [20]. (Fig. 1C); however, over-expression of GST-RIG-I747-801 suppressed reporter gene activation upon viral stimulus, suggesting that the newly defined repression domain is capable of acting in *trans*, the feature described for a.a. 735–925. The secondary structure prediction program (Section 2) suggested that a.a. 747–801 is mostly composed of α-helix (Fig. 1D). Alignment of the primary sequence corresponding to linkers of LGP and RIG-I from different species revealed that several amino acids are highly conserved (Fig. 1E); notably, φXXφQ motif (in which φ is I, L or V) is conserved at a.a. 765 and 780 (human RIG-I numbering). We constructed mutants in which each of the motif was disrupted: mutant 1 (ILQ/765, 768, and 769/AAA) and mutant 2 (IIQ/780, 783, and 784/AAA), and analyzed their basal activity. Interestingly, both mutant 1 and 2 promoted reporter gene expression without viral infection (Fig. 1B), consistent with the hypothesis that the linker structure is critical for repression function.

3.2. ATP binding site of RIG-I is required for virus-induced activation of IFN-β promoter but not for constitutive activity of the linker mutants

Because the ATP binding site is indispensable for virus-induced activation of RIG-I [5], we examined whether the constitutive active RIG-I mutants described in Fig. 1B are similarly dependent on ATP binding. We introduced K270A mutation into each of the deletions, mutant 1 and 2 and examined their activity (Fig. 1F). Interestingly, KA mutation did not change the trans-activation potential of the constitutive active mutants. As expected, K270A mutation totally abolished SeV-induced activation of IFN-β promoter by wt RIG-I (Fig. 1G). On the other hand, although mutant 1 and 2 are constitutively active, their activation level was not enhanced by SeV infection in K270 or K270A context. To further confirm whether the constitutive active mutants activate the reporter gene through the activation of IRF-3, we examined IRF-3 dimerization in cells over-expressing wt and mutants (Fig. 2). IRF-3 dimer formation was observed in cells over-expressing constitutively active mutants 1-770, 1-746 and 1-734 (Fig. 2A), and the level of IRF-3 dimer was roughly proportional to the reporter assay (Fig. 1B). Likewise, mutant 1 and 2 induced IRF-3 dimer (Fig. 2B).

3.3. Mutation 1 and 2 within the linker did not affect RNA binding activity of RIG-I

Next, the RNA binding activity of RIG-I mutant 1 and 2 was examined using 25 bp dsRNA (p25/25), 5′ tri-phosphate-containing RNA (5′pppGG25), and poly (I:C) (Fig. 3A and B). Wild-type RIG-I, and mutant 1 and 2 exhibited binding to these RNA. Mutant 1 and 2 bound to 5′ pppGG25 and poly (I:C) with slightly increased efficiency (in repeated experiments, data not shown). These results suggest that mutation within the linker did not cause overall structural distortion and at least preserved the function of RNA recognition.

3.4. Mutation 1 and 2 within the linker disconnected dsRNA binding and ATPase activity of RIG-I

Wild-type RIG-I, and mutant 1 and 2 were produced as GST fusion, purified and subjected to the ATPase assay (Section 2). Although wild-type RIG-I exhibited very low ATPase activity, it was markedly enhanced by 5′ pppGG25 or poly (I:C) (Fig. 3C). In contrast, ATPase activity of mutant 1 and 2 was not increased even

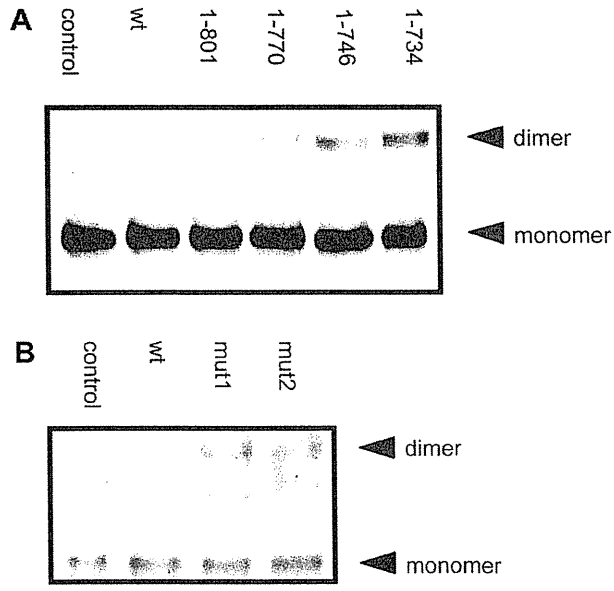

Fig. 2. Linker region of RIG-I regulates the activation of IRF-3. Dimerization of IRF-3 induced by RIG-I mutants. Huh7.5 cells were transfected with empty vector (control), expression vector for Flag-tagged RIG-I wt or indicated mutants. 36 h (A) or 16 h (B) after transfection, cell lysates were subjected to Native PAGE and immunoblot analysis with anti-IRF-3 antibody. IRF-3 monomer and dimer are indicated by arrows.

Please cite this article in press as: M. Kageyama et al., 55 Amino acid linker between helicase and carboxyl terminal domains of RIG-I functions as a critical repression domain and determines inter-domain conformation, Biochem. Biophys. Res. Commun. (2011), doi:10.1016/j.bbrc.2011.10.015

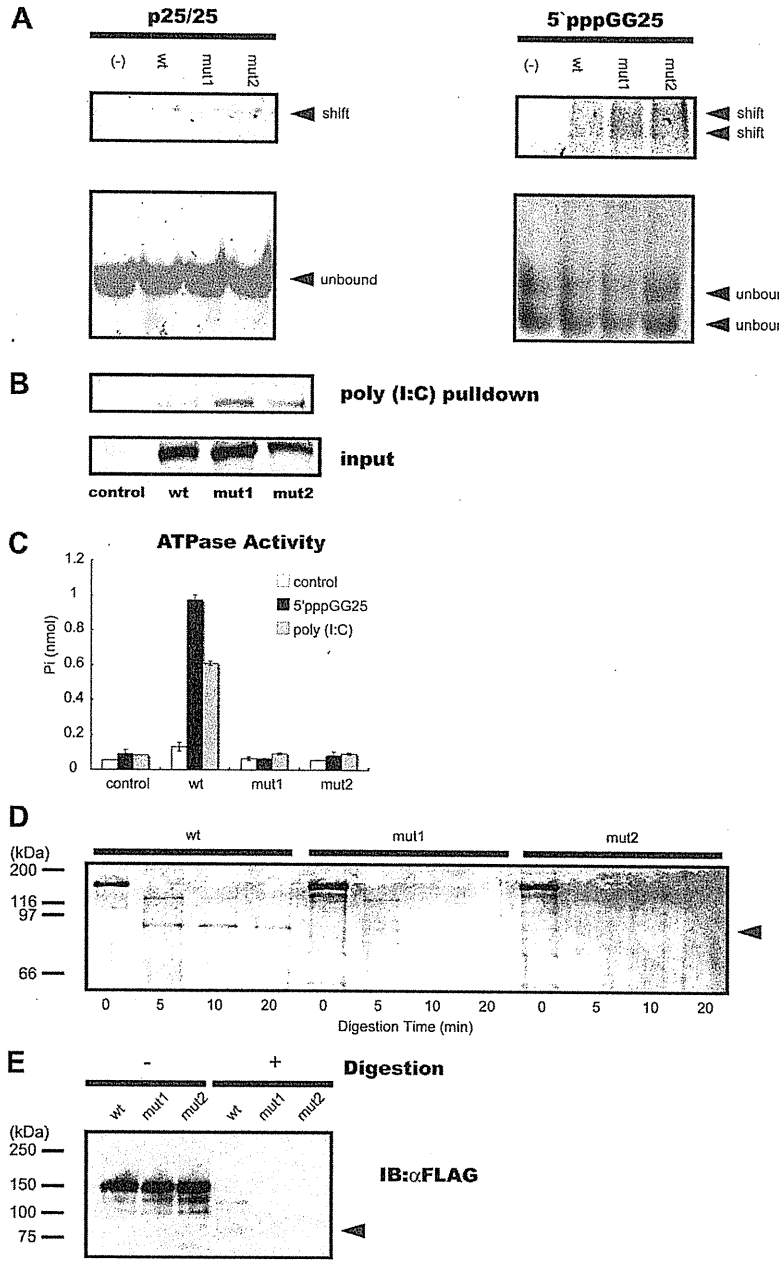

Fig. 3. Characterization of RIG-I mutant protein. (A) RNA-binding activity of RIG-I wt and mutants. Recombinant full-length RIG-I was incubated with p25/25 (left) or 5'pppGG25 (right) and separated by gel electrophoresis (Section 2). Arrows denote the position of unbound RNA (lower) or RNA-RIG-I complex (upper). (B) Poly (I:C) pull-down of RIG-I proteins. Extract from HEK293T cells transfected with empty vector (control), Flag-tagged RIG-I wt or mutant vectors was mixed with poly (I:C)-agarose beads, and subjected to pull-down assay. RIG-I proteins in the input material (lower panel) and recovered from pull-down (upper panel) are shown. (C) ATPase activity of RIG-I. ATPase activity of the recombinant GST-RIG-I proteins was determined as described in Section 2. Data are the mean ± SD ($n = 2$). Similar data were obtained from a separate experiment. (D and E) protease digestion of RIG-I. Recombinant GST-RIG-I proteins were digested with trypsin at 37 °C for the indicated times, resolved by SDS–PAGE and visualized by silver staining (D). Similarly digested RIG-I (for 20 min) was analyzed by immunoblotting with anti-Flag (E).

in the presence of ligands. As both mutant 1 and 2 bind dsRNA similarly to the wild-type (Fig. 3A and B), these mutants are incapable of connecting the dsRNA binding signal to the activation of ATPase. These results suggest that mutation 1 and 2 result in altered conformation of RIG-I.

3.5. Conformational change of RIG-I induced by mutation 1 and 2

To investigate the conformational change of RIG-I, we subjected wild-type RIG-I and mutants to limited trypsin digestion and analyzed the digested product by SDS–PAGE (Fig. 3D). Trypsin digestion of wild-type RIG-I generated an intermediate RIG-I fragment of 90 kD after 5 min of digestion. This fragment persisted at least until 20 min of digestion, suggesting that it is relatively resistant to this protease. Western blotting using anti-Flag antibody, whose epitope is attached at the amino terminus of the RIG-I construct, revealed that the 90 kD fragment contains the intact Flag epitope attached to the N-terminus of RIG-I (Fig. 3E). Notably, the result suggests that the CARD was protected from digestion. From the calculated molecular mass of the fragment, we mapped the cleav-

Please cite this article in press as: M. Kageyama et al., 55 Amino acid linker between helicase and carboxyl terminal domains of RIG-I functions as a critical repression domain and determines inter-domain conformation, Biochem. Biophys. Res. Commun. (2011), doi:10.1016/j.bbrc.2011.10.015

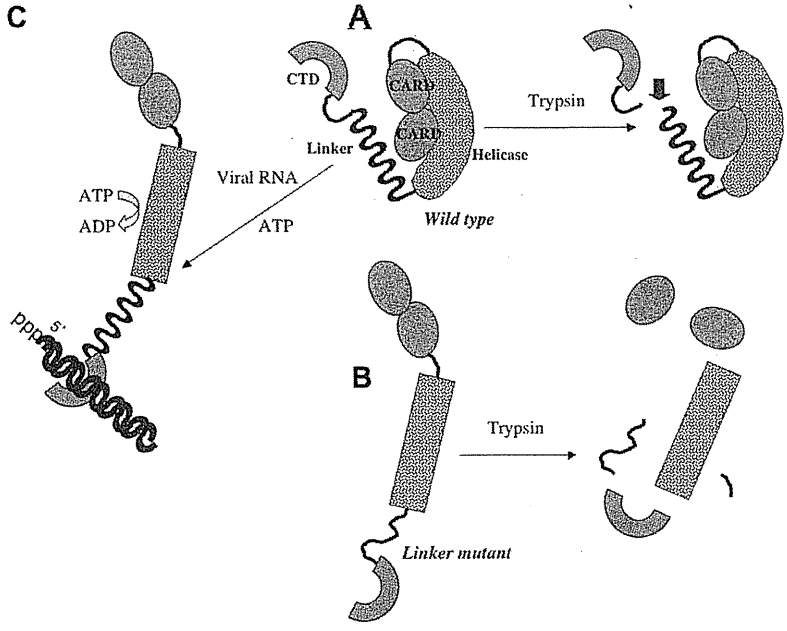

Fig. 4. Model for basal repression and de-repression of RIG-I. Schematic model of RIG-I suppression by its linker region and de-repression by viral RNA is shown. Tandem CARDs and domains encoding the helicase, linker and CTD are shown. The linker repressed RIG-I signaling by masking CARDs in the absence of viral RNA (A). Trypsin digestion partially digested RIG-I, resulting in digestion-resistant fragment consisting of CARD and helicase domain. Linker mutation changes the linker structure, resulting in the open conformation, in which CARD is exposed (B). Mutant 1 and 2 were highly sensitive to trypsin digestion and no resistant fragment was observed. Binding of viral RNA to RIG-I induces ATPase activity, leading to its conformational change, resulting in unmasking of CARD (C).

age site around amino acid 800 of RIG-I and GST was cleaved off. In sharp contrast, neither mutant 1 and 2 exhibited a trypsin-resistant fragment within this range of digestion, strongly suggesting that the conformation of mutant 1 and 2, particularly the complex of CARD and helicase domain, is much less resistant to trypsin digestion.

4. Discussion

In the present work, we demonstrated that the linker, which connects the helicase domain and CTD, is the minimal domain for the repression of constitutive activity of RIG-I. Prediction of the secondary structure suggested that the linker is mostly composed of α-helix. Furthermore, comparison of the primary sequences of the linkers of RIG-I and LGP2 proteins revealed conserved amino acid residues. Mutagenesis of these key amino acids resulted in impaired repression function. We hypothesized a model, described in Fig. 4. Wild-type RIG-I conforms a closed structure so CARD is masked (Fig. 4A); thus, the basal activity of wild-type RIG-I is minimized. Mutation of the linker disrupts the closed conformation and results in the release of CARD. The protease digestion of wild-type and mutant RIG-I strongly suggests a conformational change by linker mutation (Fig. 4B). Interestingly, once such a conformational change is allowed by mutation, ATPase activity is dispensable for signaling (Fig. 1F). This is consistent with the hypothesis that RIG-I CARD is essential for signaling but its availability is strictly regulated by the overall conformation of full-length RIG-I. Our protease digestion experiment demonstrates for the first time that two distinct conformations, repressed (wild-type RIG-I) and de-repressed (mutant RIG-I) exist and that the linker of 55 amino acids is responsible for autorepression.

The autorepression state can be reversed by viral infection through a multiple step mechanism: (i) recognition of non-self RNA, (ii) binding and hydrolysis of ATP, (iii) conformational change and (iv) ubiquitination. The non-self RNA patterns, such as dsRNA and 5′tri-phosphate are recognized by the CTD and helicase domain [10]. RNA binding induces ATPase activity of RIG-I (Fig. 3C), leading to the conformational change (Fig. 4C). In addition, there are several reports that ubiquitination plays an important role in RIG-I activation, although the proposed models are not consistent [21–23]. It is therefore important to determine the repressed and de-repressed conformation of full-length RIG-I at atomic resolution. Such structures will explain how the linker region regulates the overall conformation of the RIG-I molecule.

Acknowledgments

We thank Pro. S. Yonehara for valuable discussion. This work was supported in part by a Grant-in-Aid from the Ministry of Education, Science, Sports and Culture, Japan, the Ministry of Health, Labor and Welfare, the PRESTO Japan Science and Technology Agency, the Uehara Memorial Foundation, Takeda Science Foundation, and Nippon Boehringer Ingelheim.

References

[1] Y.M. Loo, M. Gale, Immune signaling by RIG-I-like receptors, Immunity 34 (2011) 680–692.
[2] M. Schlee, G. Hartmann, The chase for the RIG-I ligand–recent advances, Mol. Ther. 18 (2010) 1254–1262.
[3] O. Takeuchi, S. Akira, Innate immunity to virus infection, Immunol. Rev. 227 (2009) 75–86.
[4] M. Yoneyama, T. Fujita, Recognition of viral nucleic acids in innate immunity, Rev. Med. Virol. 20 (2010) 4–22.
[5] M. Yoneyama, M. Kikuchi, T. Natsukawa, N. Shinobu, T. Imaizumi, M. Miyagishi, K. Taira, S. Akira, T. Fujita, The RNA helicase RIG-I has an essential function in double-stranded RNA-induced innate antiviral responses, Nat. Immunol. 5 (2004) 730–737.
[6] M. Yoneyama, M. Kikuchi, K. Matsumoto, T. Imaizumi, M. Miyagishi, K. Taira, E. Foy, Y.M. Loo, M. Gale, S. Akira, S. Yonehara, A. Kato, T. Fujita, Shared and unique functions of the DExD/H-box helicases RIG-I, MDA5, and LGP2 in antiviral innate immunity, J. Immunol. 175 (2005) 2851–2858.
[7] V. Hornung, J. Ellegast, S. Kim, K. Brzózka, A. Jung, H. Kato, H. Poeck, S. Akira, K.K. Conzelmann, M. Schlee, S. Endres, G. Hartmann, 5′-Triphosphate RNA is the ligand for RIG-I, Science 314 (2006) 994–997.

Please cite this article in press as: M. Kageyama et al., 55 Amino acid linker between helicase and carboxyl terminal domains of RIG-I functions as a critical repression domain and determines inter-domain conformation, Biochem. Biophys. Res. Commun. (2011), doi:10.1016/j.bbrc.2011.10.015

[8] A. Pichlmair, O. Schulz, C.P. Tan, T.I. Näslund, P. Liljeström, F. Weber, C. Reis e Sousa, RIG-I-mediated antiviral responses to single-stranded RNA bearing 5′-phosphates, Science 314 (2006) 997–1001.

[9] T. Saito, R. Hirai, Y. Loo, D. Owen, C. Johnson, S. Sinha, S. Akira, T. Fujita, M.J. Gale, Regulation of innate antiviral defenses through a shared repressor domain in RIG-I and LGP2, Proc. Natl. Acad. Sci. USA 104 (2007) 582–587.

[10] K. Takahasi, M. Yoneyama, T. Nishihori, R. Hirai, H. Kumeta, R. Narita, M.J. Gale, F. Inagaki, T. Fujita, Nonself RNA-sensing mechanism of RIG-I helicase and activation of antiviral immune responses, Mol. Cell 29 (2008) 428–440.

[11] S. Cui, K. Eisenächer, A. Kirchhofer, K. Brzózka, A. Lammens, K. Lammens, T. Fujita, K. Conzelmann, A. Krug, K. Hopfner, The C-terminal regulatory domain is the RNA 5′-triphosphate sensor of RIG-I, Mol. Cell 29 (2008) 169–179.

[12] T. Kawai, K. Takahashi, S. Sato, C. Coban, H. Kumar, H. Kato, K. Ishii, O. Takeuchi, S. Akira, IPS-1, an adaptor triggering RIG-I- and Mda5-mediated type I interferon induction, Nat. Immunol. 6 (2005) 981–988.

[13] R.B. Seth, L. Sun, C.K. Ea, Z.J. Chen, Identification and characterization of MAVS, a mitochondrial antiviral signaling protein that activates NF-kappaB and IRF 3, Cell 122 (2005) 669–682.

[14] L.G. Xu, Y.Y. Wang, K.J. Han, L.Y. Li, Z. Zhai, H.B. Shu, VISA is an adapter protein required for virus-triggered IFN-beta signaling, Mol. Cell 19 (2005) 727–740.

[15] E. Meylan, J. Curran, K. Hofmann, D. Moradpour, M. Binder, R. Bartenschlager, J. Tschopp, Cardif is an adaptor protein in the RIG-I antiviral pathway and is targeted by hepatitis C virus, Nature 437 (2005) 1167–1172.

[16] K. Honda, A. Takaoka, T. Taniguchi, Type I interferon gene induction by the interferon regulatory factor family of transcription factors, Immunity 25 (2006) 349–360.

[17] J.D. Thompson, T.J. Gibson, F. Plewniak, F. Jeanmougin, D.G. Higgins, The CLUSTAL_X windows interface. flexible strategies for multiple sequence alignment aided by quality analysis tools, Nucleic Acids Res. 25 (1997) 4876–4882.

[18] C. Combet, C. Blanchet, C. Geourjon, G. Deléage, NPS@: network protein sequence analysis, Trends Biochem. Sci. 25 (2000) 147–150.

[19] T. Iwamura, M. Yoneyama, K. Yamaguchi, W. Suhara, W. Mori, K. Shiota, Y. Okabe, H. Namiki, T. Fujita, Induction of IRF-3/-7 kinase and NF-kappaB in response to double-stranded RNA and virus infection: common and unique pathways, Genes Cells 6 (2001) 375–388.

[20] H. Kato, S. Sato, M. Yoneyama, M. Yamamoto, S. Uematsu, K. Matsui, T. Tsujimura, K. Takeda, T. Fujita, O. Takeuchi, S. Akira, Cell type-specific involvement of RIG-I in antiviral response, Immunity 23 (2005) 19–28.

[21] M. Gack, Y. Shin, C. Joo, T. Urano, C. Liang, L. Sun, O. Takeuchi, S. Akira, Z. Chen, S. Inoue, J. Jung, TRIM25 RING-finger E3 ubiquitin ligase is essential for RIG-I-mediated antiviral activity, Nature 446 (2007) 916–920.

[22] T. Shigemoto, M. Kageyama, R. Hirai, J. Zheng, M. Yoneyama, T. Fujita, Identification of loss of function mutations in human genes encoding RIG-I and mda5: Implications for resistance to type I diabetes, J. Biol. Chem. (2009).

[23] H. Oshiumi, M. Miyashita, N. Inoue, M. Okabe, M. Matsumoto, T. Seya, The ubiquitin ligase Riplet is essential for RIG-I-dependent innate immune responses to RNA virus infection, Cell Host Microbe 8 (2010) 496–509.

Please cite this article in press as: M. Kageyama et al., 55 Amino acid linker between helicase and carboxyl terminal domains of RIG-I functions as a critical repression domain and determines inter-domain conformation, Biochem. Biophys. Res. Commun. (2011), doi:10.1016/j.bbrc.2011.10.015

THE JOURNAL OF BIOLOGICAL CHEMISTRY VOL. 286, NO. 29, pp. 26210–26219, July 22, 2011

Retinoic Acid-inducible Gene I-inducible miR-23b Inhibits Infections by Minor Group Rhinoviruses through Down-regulation of the Very Low Density Lipoprotein Receptor*[S]

Received for publication, February 10, 2011, and in revised form, June 2, 2011 Published, JBC Papers in Press, June 3, 2011, DOI 10.1074/jbc.M111.229856

Ryota Ouda[‡§], Koji Onomoto[‡], Kiyohiro Takahasi[‡¶], Michael R. Edwards[‖‡‡], Hiroki Kato[‡], Mitsutoshi Yoneyama[§§¶¶], and Takashi Fujita[‡§1]**

*From the [‡]Laboratory of Molecular Genetics, Institute for Virus Research, and the [§]Laboratory of Molecular Cell Biology, Graduate School of Biostudies, Kyoto University, Kyoto 606-8507, Japan, the [¶]Institute for Innovative NanoBio Drug Discovery and Development, Graduate School of Pharmaceutical Science, Kyoto University, Kyoto 606-8501, Japan, the [§§]Medical Mycology Research Center, Chiba University, Chiba 260-8673, Japan, the [¶¶]PRESTO Japan Science and Technology Agency, Saitama 332-0012, Japan, the [‖]Department of Respiratory Medicine, National Heart and Lung Institute, Imperial College London, London SW7 2AZ, United Kingdom, the **MRC and Asthma UK Centre in Allergic Mechanisms of Asthma, London SE1 9RT, United Kingdom, and the [‡‡]Centre for Respiratory Infection, London SW7 2AZ, United Kingdom*

In mammals, viral infections are detected by innate immune receptors, including Toll-like receptor and retinoic acid inducible gene I (RIG-I)-like receptor (RLR), which activate the type I interferon (IFN) system. IFN essentially activates genes encoding antiviral proteins that inhibit various steps of viral replication as well as facilitate the subsequent activation of acquired immune responses. In this study, we investigated the expression of non-coding RNA upon viral infection or RLR activation. Using a microarray, we identified several microRNAs (miRNA) specifically induced to express by RLR signaling. As suggested by Bioinformatics (miRBase Target Data base), one of the RLR-inducible miRNAs, miR-23b, actually knocked down the expression of very low density lipoprotein receptor (VLDLR) and LDLR-related protein 5 (LRP5). Transfection of miR-23b specifically inhibited infection of rhinovirus 1B (RV1B), which utilizes the low density lipoprotein receptor (LDLR) family for viral entry. Conversely, introduction of anti-miRNA-23b enhanced the viral yield. Knockdown experiments using small interfering RNA (siRNA) revealed that VLDLR, but not LRP5, is critical for an efficient infection by RV1B. Furthermore, experiments with the transfection of infectious viral RNA revealed that miR-23b did not affect post-entry viral replication. Our results strongly suggest that RIG-I signaling results in the inhibitions of infections of RV1B through the miR-23b-mediated down-regulation of its receptor VLDLR.

Among the viral components that trigger the antiviral responses of a host, nucleic acids have been considered critical. In invertebrates and plants, the RNA interference (RNAi) system, which destroys non-self RNA in a sequence-dependent manner, is the major antiviral mechanism (1–3). In mammals, certain RNA structures rather than primary sequences are sensed as non-self to initiate a series of antiviral programs including the activation of type I IFN genes. There are at least two receptor systems functioning as sensors to detect viral RNA signatures: the endosomal Toll-like receptor (TLR)[2] 3 and TLR7/8, which interact with extracellular viral RNA (4), and the cytosolic RIG-I, melanoma differentiation associated gene 5 and laboratory of genetics and physiology 2, collectively termed the RLR (5, 6), which sense intracellular viral RNA with a double-stranded and/or 5′-triphosphate structure (7). Signaling generated by the innate immune receptors is transduced through networks with various adaptor molecules and results in the activation of IFN genes (8–10). IFN is secreted, thus expanding the antiviral signal to other cells through physical interaction with cell surface receptors thereby activating the IFN-stimulated genes (ISGs) (11). Several ISGs execute antiviral activity by inhibiting viral transcription, translation, viral assembly, and release of viral particles from the cells. Another feature of the IFN system is that it is tightly regulated by positive and negative feedback loops (12).

Although the RNAi system is operative in mammals, the IFN system appears to dominate the antiviral immune response. Recently, non-coding RNA known as miRNA has received much attention for its post-transcriptional regulation of gene expression (13, 14). Over 500 miRNA-encoding genes, which are exclusively transcribed by RNA polymerase II, have been identified in mammals. These primary miRNAs are processed by the enzyme Drosha into hairpin loop-containing pre-miRNAs, which are then subjected to export from the nucleus to cytoplasm via exportin 5 (15). Further enzymatic processing of the pre-miRNAs by Dicer leads to generation of a mature

* This work was supported in part by a Grant-in-aid from the Ministry of Education, Science, Sports and Culture in Japan, the Ministry of Health, Labor, and Welfare, the PRESTO Japan Science and Technology Agency, the Uehara Memorial Foundation, the Mochida Memorial Foundation for Medical and Pharmaceutical Research, and Nippon Boehringer Ingelheim.
[S] The on-line version of this article (available at http://www.jbc.org) contains supplemental Figs. S1–S4.
[1] To whom correspondence should be addressed: Laboratory of Molecular Genetics, Institute for Virus Research, Kyoto University, Kyoto 606-8507, Japan. Tel./Fax: 81-75-751-4031; E-mail: tfujita@virus.kyoto-u.ac.jp.

[2] The abbreviations used are: TLR, Toll-like receptor; RIG-I, retinoic acid-inducible gene I; LGP2, laboratory of genetics and physiology 2; VLDLR, very low density lipoprotein receptor; LRP, LDLR-related protein; SeV, Sendai virus; NDV, Newcastle disease virus; VSV, vesicular stomatitis virus; EMCV, encephalomyocarditis virus; RV, rhinovirus; ISG, IFN-stimulated gene; CARD, caspase recruitment domain; IRF, IFN regulatory factor; NP, nucleocapsid protein; ICAM-1, intercellular adhesion molecule 1.

miRNA duplex that is loaded into the RNA-induced silencing complex, which is then guided by the miRNA to complementary messenger RNAs. Notably, the sequence complementary in the 6–8-base pair "seed region" at the 5′ end of the miRNA seems to determine the specificity of miRNA-target mRNA interaction (16, 17).

Accumulated information has revealed that some miRNAs are involved in immune regulation. Expression profiling showed that stimulation of monocytes with lipopolysaccharide (LPS) induced the expression of miR-146. miR-146 targets tumor necrosis factor receptor-associated factor 6 (*Traf6*) and interleukin-1 receptor-associated kinase 1(*Irak1*), encoding components of the TLR signaling pathway, suggesting a negative feedback loop (18). Furthermore, liver-specific miR-122 contributes to the liver tropism of the hepatitis C virus by accelerating the binding of ribosomes to the viral RNA and hence aiding translation (19–21). These reports highlight the importance of understanding the function of miRNAs.

In this report, we examined miRNA expression upon RIG-I signaling and identified 37 miRNAs. Among them, miR-23b exhibited antiviral activity to rhinovirus (RV) 1B. RV, a member of the family *Picornaviridae*, causes an extensive range of human respiratory disorders including the common cold, viral bronchiolitis, and exacerbations of asthma and chronic obstructive pulmonary disease (22–26). Recently, primary human bronchial epithelial cells from asthmatics were found to be defective in IFN-β and IFN-λ mRNA and protein, (27, 28), providing a likely explanation for the increased vulnerability to virus-induced asthma exacerbations. Furthermore, it was revealed that TLR3, RIG-I, and melanoma differentiation associated gene 5 were important for RV-inducing innate responses (29–31). Our analyses revealed that miR-23b blocks infections of RV1B through down-regulation of its receptor, VLDLR. This is a novel antiviral mechanism activated by RIG-I signaling.

EXPERIMENTAL PROCEDURES

Cell Culture—HeLa cells were maintained in Dulbecco's modified Eagle's medium with fetal bovine serum and penicillin-streptomycin (100 units/ml and 100 μg/ml, respectively). L929 cells were maintained in minimum essential medium with fetal bovine serum and penicillin-streptomycin (50 units/ml and 100 μg/ml, respectively).

miRNA Microarray—Total RNA was isolated using TRIzol (Invitrogen) and miRNA was purified with a PureLink miRNA Isolation Kit (Invitrogen). The purified miRNA was labeled using Label IT miRNA Labeling Kits (Mirus). Hybridization was performed, using a three-dimensional gene miRNA Oligo Chip (TORAY).

Viral Infection—Cells were treated with the culture medium ("mock-treated") or infected with SeV, NDV, VSV, EMCV, RV16, or RV1B in serum-free and antibiotic-free medium. After adsorption for 1 h at 37 °C, the medium was changed and infection was continued for 24 h in the presence of serum-containing DMEM.

Treatment with Interferon-β (IFN-β)—HeLa cells were maintained in 12-well plates in the presence of serum-containing DMEM. Recombinant human IFN-β (1000 units/ml) was added to each well.

Plaque Assay—L929 cells were seeded in 24-well plates (2.5×10^5 cells/well) in minimal essential medium with 5% FBS for 24 h at 37 °C. After cell propagation, the growth medium was removed and serial dilutions of viral supernatants in serum-free and antibiotic-free minimal essential medium were added to the wells. The inoculated cells were further incubated to allow adsorption of the virus for 1 h at 37 °C. Subsequently, a mixture of agar overlay was added and the plates were incubated at 37 °C for 24 h. The plaques were visualized by staining with a 0.02% neutral red solution. The viral titer is expressed as plaque forming units.

Transfection of miR-23b and Anti-miR-23b—Double-stranded RNA oligonucleotides representing mature sequences that mimic endogenous miR-23b and anti-miR-23b (Ambion) were transfected into HeLa cells with RNAi MAX (Invitrogen) according to the manufacturer's instructions. Silencer negative control #2 small interfering RNA (Ambion) at the same concentration as miR-23b and anti-miR-23b was used in each experiment.

Real-time PCR—Total RNA was isolated using TRIzol (Invitrogen). Real-time PCR for miR-23b, -24, and -27b was performed using the TaqMan MicroRNA Reverse Transcription Kit (Applied Biosystems) according to the manufacturer's protocol. Normalization was performed by using RNU48 primers and probes. Real-time PCR was performed using TaqMan Gene Expression Assay probes for IFN-β and IL-6. The 18S rRNA gene was used as an internal control to normalize differences in each sample. The expression levels for each gene were assessed relative to the expression of 18S rRNA. Real-time PCR for RV RNA was performed using the following primers and probe: RV forward, 5-GTGAAGAGCCSCRTGTGCT-3, RV reverse, 5-GCTSCAGGGTTAAGGTTAGCC-3, RV probe, 5-TGAGTC-CTCCGGCCCCTGAATG-3.

Amido Black Staining—Cells were washed in PBS three times and fixed with methanol. 0.5% Amido Black solution was added and incubated 20 min at RT. After 20 min, the Amido Black solution was removed and eluted by 0.1 M NaOH. 630 nm absorption was measured.

$TCID_{50}$—The RV1B titer was measured by the Reed-Muench method (43).

Small Interfering RNA (siRNA) Knockdown of VLDLR and LRP5—siRNA for VLDLR (Digital Biology) and siRNA for LRP5 (IDT) were transfected into HeLa cells with RNAi MAX (Invitrogen) according to the manufacturer's instructions. Negative control siRNA (Digital Biology) at the same concentration as siVLDLR and siLRP5 was used in each experiment.

Immunoblotting—Cells were lysed with Nonidet P-40 lysis buffer (50 mM Tris (pH 8), 150 mM NaCl, and 1% Nonidet P-40). The lysate was resolved by SDS-PAGE (30 μg of protein/lane). Proteins were transferred to a nitrocellulose membrane. The membrane was blocked in 5% milk for 30 min at room temperature and probed with mouse anti-SeV Nucleocapsid protein, mouse anti-NDV Nucleocapsid protein, mouse anti-VLDLR (Santa Cruz sc-18824), or rabbit anti-LRP5 (Cell Signaling D23F7). Ab binding was detected with alkaline phosphatase-conjugated anti-mouse or anti-rabbit IgG.

RV Genomic RNA Isolation and Transfection—RV-containing medium was centrifuged at 10,000 × *g* for 24 h. The pellet

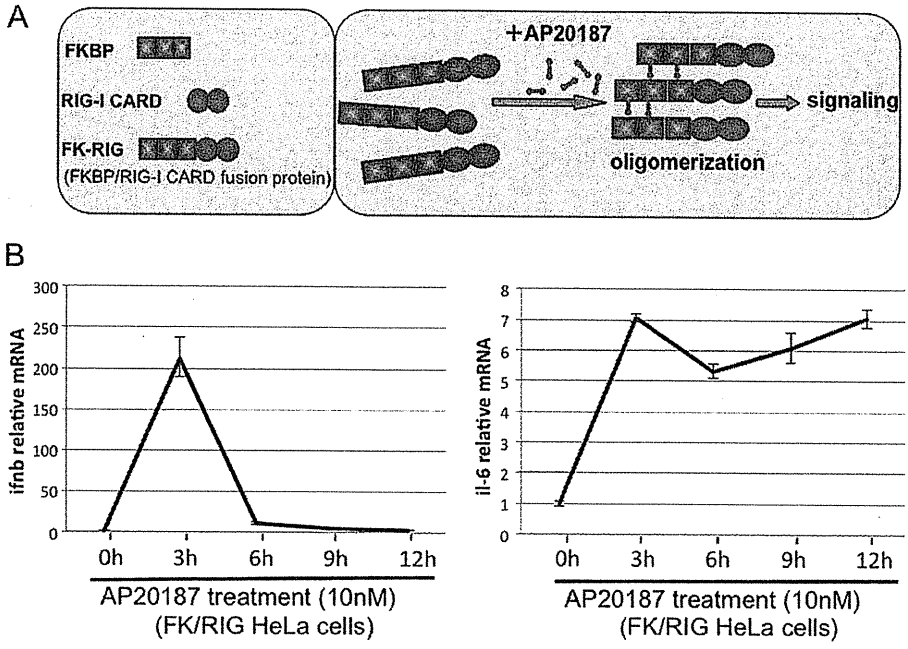

FIGURE 1. **Artificial oligomerization of the CARD of RIG-I results in signaling to activate the IFN-β and IL-6 genes.** *A*, schematic representation of the FK/RIG fusion protein and its oligomerization by a cross-linking reagent, AP20187. *B*, HeLa cells stably expressing FK/RIG were treated with AP for the period indicated and cells were harvested to examine endogenous IFN-β and IL-6 mRNA levels by real-time PCR.

was suspended in TRIzol (Invitrogen). The RV genomic RNA (0.5 μg) and miR-23b were transfected into HeLa cells with Lipofectamine 2000 (Invitrogen).

Statistical Analysis—Statistical analysis were conducted with an unpaired *t* test, with values of $p < 0.05$ considered statistically significant. Each point in a graph represents the mean ± S.E. for at least three independent experiments.

RESULTS

Induction of miRNA Expression by RIG-I Signaling—To directly examine the impact of the activation of RIG-I on the gene expression profile, we developed an artificial RIG-I activation system (details will be reported elsewhere).[3] Briefly, the N-terminal signaling domain of RIG-I, caspase recruitment domain (CARD), was introduced into the ARGENT™ Regulated Homodimerization Kit (ARIAD). The resultant FKBP/RIG-I CARD fusion protein (FK/RIG) allowed CARD to oligomerize by the chemical compound, AP20187 (AP), and to introduce CARD-mediated signaling into the cells (Fig. 1*A*). As shown in Fig. 1*B*, the endogenous mRNA levels of IFN-β and IL-6 in HeLa cells stably expressing FK/RIG (HeLa FK/RIG) were significantly increased by the enforced oligomerization of RIG-I CARD (Fig. 1*B*). Furthermore, microarray analyses of the transcripts of these cells revealed transient expression of IFN genes and ISGs with a concomitant induction of IFN regulatory factor (IRF-3) dimerization and NF-κB DNA-binding activity (data not shown). Thus we concluded that the FK/RIG system could mimic the virus-induced activation of RIG-I signaling.

To analyze the miRNA expression profile in HeLaFK/RIG cells, RNA fractions were prepared at 3, 6, 9, and 12 h after the addition of AP and subjected to analysis with a miRNA

[3] K. Onomoto, M. Yoneyama, and T. Fujita, unpublished data.

TABLE 1
miRNA induced by RIG-I-mediated signaling

HeLa cells stably expressing FK/RIG were treated with AP for the periods indicated and miRNA expression was determined by miRNA microarray (*TORAY*). The relative expression (fold-increase compared to the baseline miRNA level at 0 h) of representative miRNA whose expression was up-regulated more than 2-fold is shown. The opposite strand of miRNA is denoted with an asterisk (*).

	AP20187 treatment (FK/RIG-HeLa cells)				
	0 h	3 h	6 h	9 h	12 h
miR-423–3p	1.00	2.31	2.77	4.34	4.59
miR-301b	1.00	2.31	UD[a]	UD	UD
miR-923	1.00	3.63	1.34	1.50	0.84
miR-181a*	1.00	UD	7.16	UD	UD
miR-23b	1.00	1.47	2.32	1.03	1.27
miR-125b	1.00	1.94	2.73	1.16	1.38
miR-505*	1.00	UD	2.41	UD	UD
miR-940	1.00	UD	2.11	UD	UD
miR-1226	1.00	0.90	2.05	UD	UD
miR-1229	1.00	UD	2.80	UD	UD
miR-1281	1.00	UD	2.21	UD	UD
miR-149	1.00	UD	0.99	3.36	UD
miR-188–5p	1.00	1.85	1.36	3.70	UD
miR-320	1.00	1.22	1.31	2.62	1.71
miR-200c	1.00	1.20	1.03	2.63	UD
miR-362–5p	1.00	1.09	0.94	5.65	UD
miR-425*	1.00	UD	UD	8.81	UD
miR-769–3p	1.00	1.00	1.01	2.65	UD
miR-801	1.00	1.09	0.92	9.18	1.27
miR-29b-1*	1.00	1.43	1.27	2.00	UD
miR-92b*	1.00	0.70	0.88	2.29	UD
miR-1225–3p	1.00	UD	UD	7.16	UD
miR-1228	1.00	UD	1.24	5.77	UD
miR-1249	1.00	UD	UD	5.89	UD
miR-1280	1.00	0.63	1.19	8.00	1.74
miR-664	1.00	1.55	UD	23.75	UD
miR-664*	1.00	1.55	UD	22.62	UD
miR-19b	1.00	1.26	1.40	1.14	2.05
miR-7i	1.00	1.42	1.50	1.68	2.92
miR-484	1.00	0.84	1.38	1.67	2.04
miR-500*	1.00	1.58	1.76	1.73	3.18
miR-421	1.00	1.61	1.90	0.96	2.11
miR-671–5p	1.00	UD	UD	UD	5.38
miR-768–5p	1.00	0.61	0.57	UD	2.94
miR-939	1.00	0.79	0.71	UD	2.75
miR-320b	1.00	1.39	1.44	1.92	2.20
miR-1304	1.00	1.69	1.9	UD	31.12

[a] UD, undetermined.

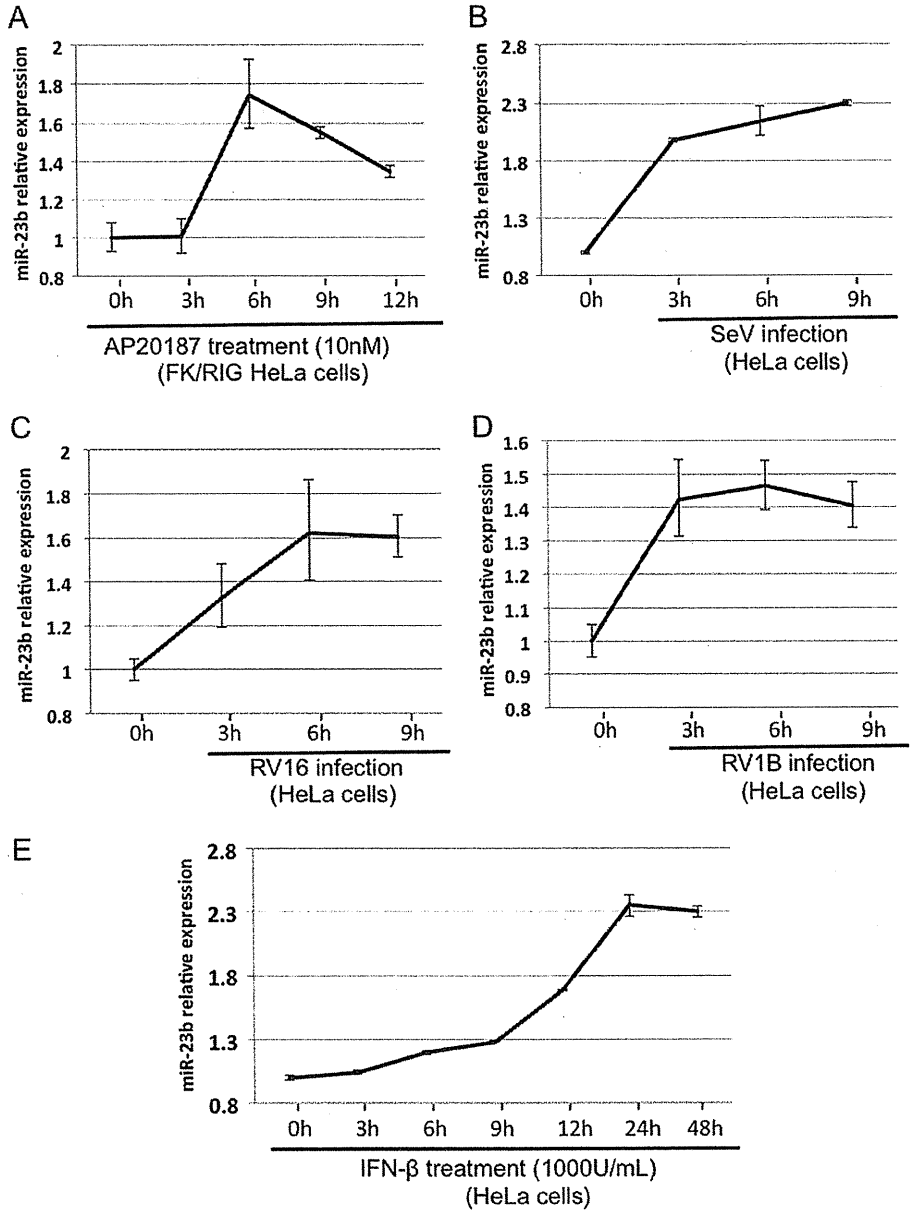

FIGURE 2. **Induction of miR-23b by RIG-I signaling, SeV and RV infection, or IFN-β treatment.** HeLa cells stably expressing FK/RIG were treated with AP (*A*). *B–E*, HeLa cells were infected with SeV (*B*), infected with RV16 (*C*), RV1B (*D*), or treated with IFN-β (1000 units/ml) (*E*). The miRNA fraction was extracted at the time points indicated and the amount of miR-23b was determined by real-time PCR.

microarray (TORAY) that covers 900 miRNAs. The expression level of several miRNAs was up- or down-regulated after the addition of AP (supplemental Fig. S1), the miRNAs exhibiting elevated levels of expression are listed in Table 1. For up-regulated miRNA, the induction kinetics appear to be different. This is commonly observed for different ISGs, presumably the induction is regulated by transcription and post-transcriptional mechanisms. Certainly this issue requires further investigation. Among these RIG-I-inducible miRNA, we focused on miR-23b because (i) it has been reported that miR-23b is regulated by NF-κB (32) and (ii) a data base search revealed that miR-23b has several target sites on mRNA encoding VLDLR (see below). To confirm the results obtained with the miRNA microarray, we monitored expression of miR-23b by real-time PCR. AP treatment resulted in a 1.7-fold increase in miR-23b at 6 h in HeLaFK/RIG with similar kinetics as in the microarray assay (Fig. 2*A*). The Sendai virus (SeV) and two strains of rhinovirus (RV16 and RV1B) also induced miR-23b accumulation (Fig. 2, *B–D*) with similar kinetics to the endogenous IFN-β mRNA expression (supplemental Fig. S2, *A–C*). miR-23b is reported to be derived from the polycistronic miRNA cluster that consists of miR-23b-27b-24 in the human gene, *C9orf3* (supplemental Fig. S3*A*) (32). As expected, the expression of miR-24 and miR-27b was also induced by RV16 and RV1B infection (supplemental Fig. S3, *B* and *C*), suggesting that these miRNA are regulated by a common mechanism. On the other hand, treatment of cells

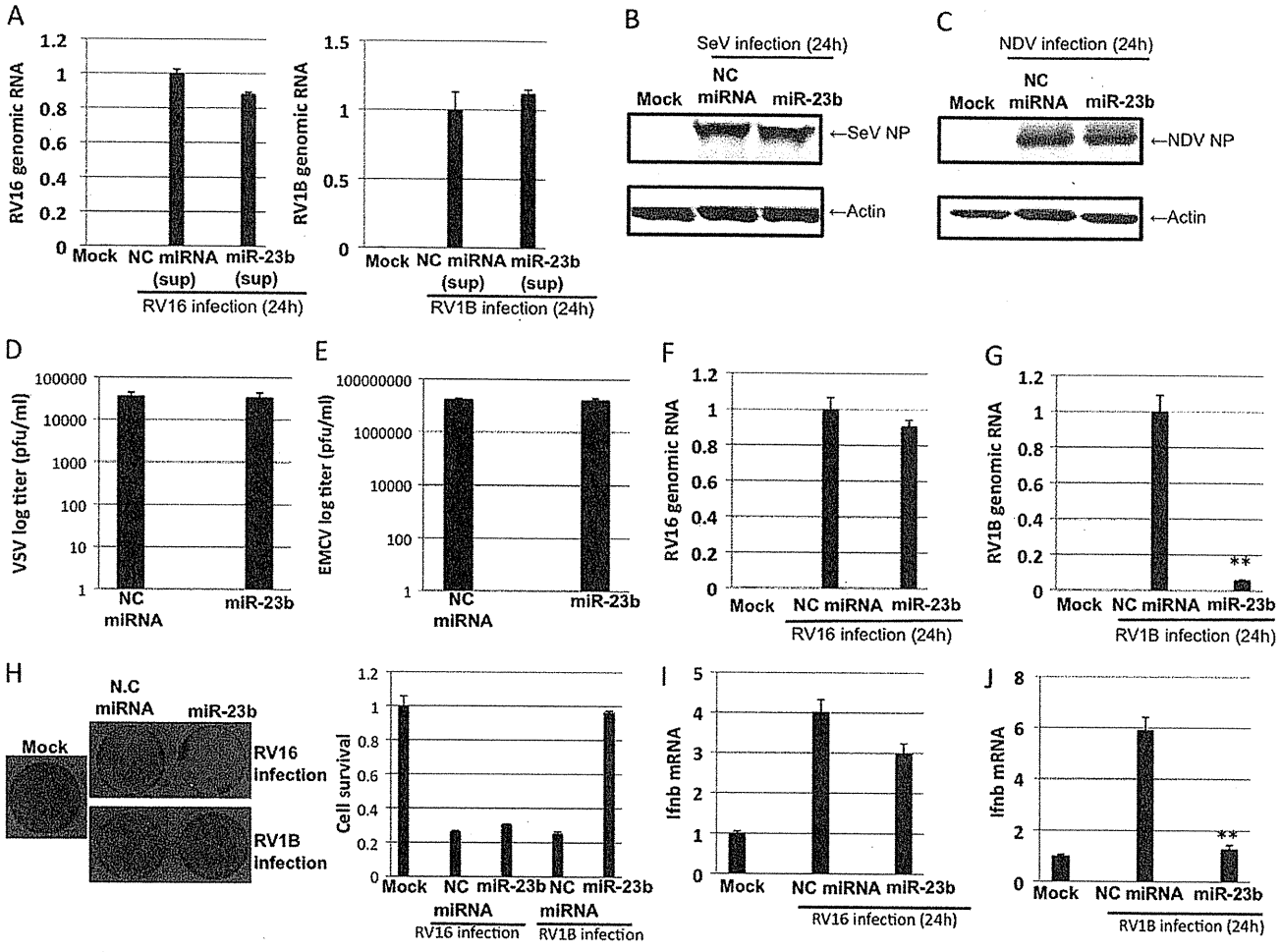

FIGURE 3. **The effect of miR-23b transfection on viral growth.** *A*, HeLa cells were transfected with negative control miRNA (*NC miRNA*) or miR-23b for 48 h, the culture supernatant (*sup*) was collected, and HeLa cells were treated with supernatant for 24 h and then infected with RV for 24 h. Levels of RV genomic RNA were determined by real-time PCR. *B-G*, HeLa cells transfected with NC miRNA or miR-23b for 48 h were infected with SeV (*B*), NDV (*C*), VSV (*D*), EMCV (*E*), RV16 (*F*), or RV1B (*G*) for an additional 24 h. The viral NP level was determined by Western blotting (*B*, SeV; *C*, NDV). Infectivity in the culture supernatant was determined by plaque assay (*D*, VSV; *E*, EMCV). Levels of RV genomic RNA were determined by real-time PCR (*F*, RV16; *G*, RV1B) using specific primer sets. *H*, Amido Black staining of miRNA-transfected and RV-infected cells. IFN-β mRNA levels of the RNA samples in *F* and *G* are shown in *I* and *J*, respectively. **, $p < 0.005$.

with IFN-β also induced miR-23b expression with a peak at 24 h, suggesting that in addition to RIG-I-mediated signaling, IFN receptor-mediated signaling induces miR-23b expression albeit with slow kinetics (Fig. 2*E*). These results suggest that, although the expression of miR-23b is up-regulated by both RIG-I- and IFN-mediated signaling, the former is mainly responsible for transient induction after oligomerization of RIG-I CARD.

Selective Effect of miR-23b on Rhinovirus 1B Replication—To examine whether miR-23b has an antiviral effect, HeLa cells were transiently transfected with synthetic miR-23b (Ambion), which is a chemically modified double-stranded RNA and mimics endogenous miR-23b, or control miRNA (NC miRNA) for 48 h and infected with SeV, Newcastle disease virus (NDV), vesicular stomatitis virus (VSV), encephalomyocarditis virus (EMCV), and two strains of rhinovirus (RV16 and RV1B) for 24 h. RV16 and RV1B are representative of major and minor group RVs, respectively, and utilize distinct cellular receptors for viral entry (33–35). First, to exclude the possibility that miRNA induces production of antiviral humoral factors such as IFNs, we examined antiviral activity in the culture supernatant of HeLa cells transfected with either control miRNA or miR23b. The supernatant did not affect viral RNA yields from RV-infected HeLa cells, indicating that miR23b does not induce production of antiviral cytokines (Fig. 3*A*). Next, we tried to examine the effect of miR-23b on viral growth. For SeV and NDV infections, nucleocapsid proteins (NPs), which are known to interact with viral genome in infected cells, were detected by Western blotting with specific antibodies (Fig. 3, *B and C*). Transfection with miR-23b did not influence the accumulation of NPs in SeV- or NDV-infected cells, suggesting no effect on growth of these viruses. In the case of VSV and EMCV, we determined viral titer from the infected cells by plaque assays (Fig. 3, *D* and *E*). Transfection with miR-23b did not influence yields of VSV or EMCV. For RV16 and RV1B, the accumulation of viral RNA was examined by real-time PCR. The introduction of miR-23b moderately reduced the amount of RV16 RNA, however, a dramatic

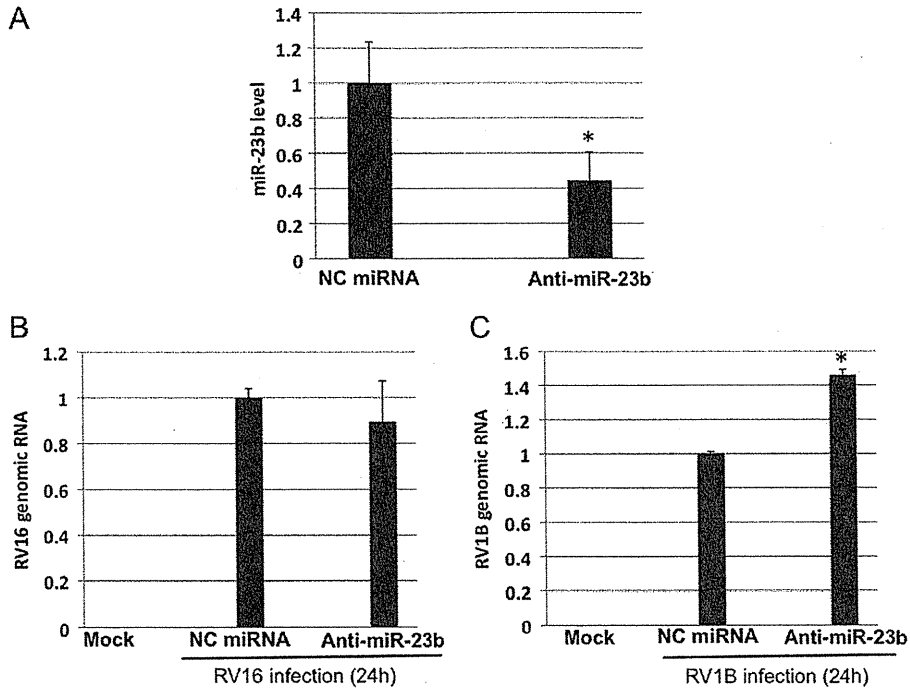

FIGURE 4. **Anti-miR-23b enhanced RNA yields of RV1B.** HeLa cells were transfected with NC miRNA or anti-miR-23b for 48 h and infected with RV for 24 h. *A*, the expression of miR-23b after anti-miR-23b transfection was determined by real-time PCR. *B* and *C*, the yield of genomic RNA of RV16 (*B*) and RV1B (*C*) was determined by real-time PCR. *, $p < 0.05$.

reduction of RV1B viral RNA was observed (Fig. 3, *F* and *G*). Furthermore, RV1B titer was severely reduced by miR-23b treatment (supplemental Fig. S4*A*). Consistent with this, the cell survival rate was significantly restored by miR-23b transfection after RV1B infection but not RV16 infection (Fig. 3*H*). Again, to verify whether the effect of miR-23b on viral RNA yield of RV1B is indirectly mediated by the secreted IFNs, endogenous IFN-β mRNA levels in miR-23b-transfected and RV-infected cells were determined (Fig. 3, *I* and *J*). In cells infected with RV16 or RV1B, IFN-β mRNA levels were closely correlated to the viral yields (compare Fig. 3, *F* and *G* to *I* and *J*, respectively), suggesting that the decrease of RV1B RNA caused by miR-23b is unlikely due to enhanced production of IFN-β. Taken together, these results suggest that miR-23b has an antiviral effect specific to RV1B.

Down-regulation of miR-23b Expression Resulted in Increased RNA Yields of RV1B—To further investigate the mechanism of the antiviral effect of miR-23b on RV1B, we transiently expressed anti-miR-23b in HeLa cells. This anti-miR-23b (Ambion) is a chemically modified single-stranded RNA and specifically bind miR-23b, inhibiting the function of miR-23b. The transfection led to a 60% decrease of endogenous miR-23b production, compared with NC-miRNA transfection (Fig. 4*A*). Under these conditions, the RV16 RNA level was not changed by anti-miR-23b (Fig. 4*B*). On the other hand, the RV1B RNA level was significantly increased by anti-miR-23b (Fig. 4*C*). Consistent with this, RV1B titer was clearly increased by anti-miR-23b transfection (supplemental Fig. S4*B*). These results further confirm that the inhibition of RV1B RNA is mediated by miR-23b.

LRP5 and VLDLR Are Targets of miR-23b—A bioinformatic-based (microRNA.org) search of databases revealed 1 and 6 target sites on mRNA encoding LDLR-related protein 5 (LRP5) and VLDLR, respectively (Fig. 5, *A* and *B*). Because it has been reported that minor group RVs, including RV1B, use LDLR family proteins (LDLR, VLDLR, and LRPs) as cellular receptors and major group RVs utilize ICAM-1, we speculate that miR-23b specifically affects expression of RV1B receptors. To confirm this, miR-23b was introduced into HeLa cells and its effect on expression of LRP5 and VLDLR was determined by Western blotting (Fig. 5). The levels of LRP5 and VLDLR were significantly reduced by transfection of miR-23b, suggesting that miR-23b targets mRNA for these proteins. Furthermore, induction of endogenous miR-23b expression through the activation of FK/RIG by AP treatment in HeLaFK/RIG cells resulted in decreased levels of LRP5 and VLDLR (Fig. 5*C*). However, anti-miR-23b blocked this reduction. These results strongly suggest that endogenous miR-23b participate in the down-regulation of LRP5 and VLDLR expression via RIG-I-mediated signaling.

Knockdown of VLDLR Reduced RV1B RNA Yields—To clarify which of the miR-23b-targeted LDLR family proteins are critical for RV1B infections, we individually knocked down LRP5 and VLDLR using specific siRNA (Fig. 6*A*) and the RV viral RNA yield was compared (Fig. 6, *B* and *C*). As expected, the viral RNA of RV16, which utilizes ICAM-1 as a receptor (36), was not affected by either siRNA treatment. However, knockdown of VLDLR dramatically reduced RV1B RNA yields. Knockdown of LRP5 enhanced RV1B RNA yields, however, this effect was not observed in cells with the double